Homogeneous Organic Reactions as Mechanistic Probes in Supercritical Fluids

Joan F. Brennecke*,† and John E. Chateauneuf*,‡

Department of Chemical Engineering, University of Notre Dame, Notre Dame, Indiana 46556, and Department of Chemistry, Western Michigan University, Kalamazoo, Michigan 49008

Received May 15, 1998 (Revised Manuscript Received November 13, 1998)

Contents

I. Introduction and Scope 433
II. Potential Ways for Solvation in Supercritical Fluids To Affect Reactivity 434
  A. Local Density Augmentation 434
  B. Preferential Solvation 435
  C. Thermodynamic Pressure Effect on the Rate Constant 435
III. Reactions That Probe Solvation in Supercritical Fluids 436
  A. Diffusion-Controlled Reactions 436
  B. Kinetically-Controlled Reactions 439
  C. Equilibrium Reactions 442
  D. SCF Solvent Cage Effects 445
  E. Other Important Reactions and Directions 450
IV. Summary 451
V. Acknowledgments 451
VI. Literature Cited 451

Joan F. Brennecke received her B.S. in Chemical Engineering (1984) from the University of Texas at Austin and her M.S. and Ph.D. (1987 and 1989) from the University of Illinois at Urbana—Champaign. She is currently Professor of Chemical Engineering at the University of Notre Dame. Her research interests include solvent effects on reactions in supercritical fluids, supercritical fluid extraction, high-pressure phase behavior, and environmentally conscious chemical processing.

John E. Chateauneuf was born on April 19, 1957, in Swampscott, MA. He received his B.S. degree in chemistry from Salem State College in 1981 and his Ph.D. in chemistry from Tufts University in 1986. He performed his postdoctoral research with K. U. Ingold as a Research Associate in the Division of Chemistry, Free Radical Chemistry Section of the National Research Council of Canada in Ottawa. In 1988, he joined the research faculty at The University of Notre Dame Radiation Laboratory, and served as head of the Organic Photochemical Processes Section. In 1996, he joined the faculty in the Department of Chemistry at Western Michigan University. His research interests include kinetic and mechanistic studies of reaction intermediates, photophysical, and photochemical processes and the development of supercritical fluids as environmentally benign reaction media.

I. Introduction and Scope

An interesting and intriguing aspect of supercritical fluid solutions is their microscopic inhomogeneities. The most well-known of these are the long-range densities fluctuations that occur in a pure fluid at conditions close to the critical point.[1] However, there are also short-range inhomogeneities around dissolved solutes in supercritical fluids, which are frequently referred to as local density augmentation and local composition enhancements. Many questions have arisen about the potential influences that short-range solvation and long-range density fluctuations might have on complex chemical reaction schemes. In attempts to answer these questions, researchers have sought to study the effect of supercritical fluid solvents on simple unimolecular and bimolecular reactions. In doing so, the reactions themselves have become probes of the molecular structure and the influence of solvation on reactivity in supercritical fluids (SCFs).

In this paper, we attempt to review those studies that involve simple reactions as probes of molecular structure and its effect on reactivity in SCFs. We have limited the review to homogeneous reactions of organic compounds and have neglected studies in near-critical and supercritical water,[2−4] which exhibit

† University of Notre Dame.
‡ Western Michigan University.

10.1021/cr970035q CCC: $35.00
Published on Web 01/09/1999

their own set of interesting physical properties. There are many important studies of reactivity in SCFs that we do not include because we have chosen to focus on ones that most clearly elucidate the effects of solvent structure. Many of these other studies are included elsewhere in this volume and in a more general review article of reactions at supercritical conditions by Savage and co-workers.[4] Also, there is a growing body of studies of organometallic reactions in SCFs,[5] many of which have contributed to our understanding of solvation and solvent effects on reactions in SCFs.

This article is divided into three sections. First, to put the kinetic studies in perspective, we discuss the ways the solvent microstructure may potentially influence reactions. Second, we review the simple homogeneous organic unimolecular and bimolecular reaction studies that have provided insight into solvation in SCFs and its effect on reactivity. Third, we summarize the results and attempt to provide a general framework in which to understand the results in terms of the reaction and solvation processes.

II. Potential Ways for Solvation in Supercritical Fluids To Affect Reactivity

The tremendous efforts to understand solvent effects on reactivity in SCFs in the past decade are largely a result of the many studies that show local environments around dissolved solutes in SCFs that are very different than the bulk. This local solvation is in addition to the long-range density fluctuations that occur in SCFs at conditions near the critical point. Since these long- and short-range phenomena are the impetus for using simple reactions to probe molecular structure in SCF solutions, we will highlight studies (mostly spectroscopic ones) of local density augmentation, local composition enhancement, and partial molar volumes in SCF solutions.

A. Local Density Augmentation

Perhaps the first observations of local density augmentation around a dilute solute in SC fluids were from the solvatochromic shifts of phenol blue.[6] Kim and Johnston[6] found that the steady-state UV−vis absorption transition energy did not follow that predicted by McRae's theory[7] based on Onsager reaction field theory due to the bulk density. In a supercritical fluid at a particular bulk density the probe molecule had an absorption transition energy that McRae's theory predicted would occur at a higher density. Johnston and co-workers interpreted these measurements as indications that the local density felt by the probe was significantly greater than the bulk density. Subsequently, Randolph and co-workers[8] have clearly shown that the maximum in the local density augmentation (ρ_{local}/ρ_{bulk}), where ρ is the density, occurs at densities well below the critical density, as shown in Figure 1. These estimates of the local density were obtained from the hyperfine splitting constant of di-*tert*-butyl nitroxide radicals measured by electron paramagnetic resonance (EPR) spectroscopy.

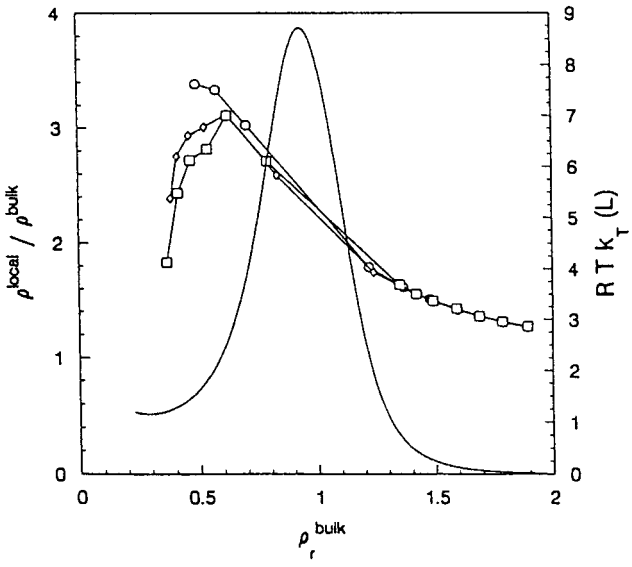

Figure 1. ρ^{local}/ρ^{bulk} vs reduced bulk density, ρ_r^{bulk}, for di-*tert*-butyl nitroxides in ethane, as measured by EPR spectroscopy. Also shown is the bulk isothermal compressibility (solid line). (Reprinted with permission from ref 8. Copyright 1993 American Institute of Chemical Engineers.)

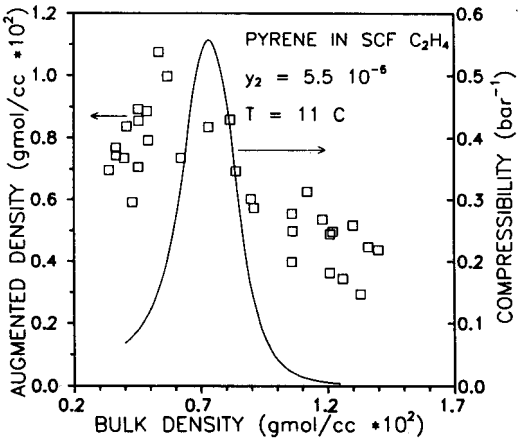

Figure 2. The augmented density (local density − bulk density) around pyrene in ethylene at 11 °C, as measured by fluorescence spectroscopy. Also shown is the bulk isothermal compressibility (solid line). (Reprinted from ref 9. Copyright 1990 American Chemical Society.)

The EPR results emphasize that local density augmentation is a result of local solvation and is not a critical phenomenon, i.e., it does not correlate with the isothermal compressibility of the solvent, which diverges at the critical point. In light of the EPR studies, it now seems clear that earlier work[6,9] also supports the conclusion that the maximum in the local density augmentation does not occur at the critical point. Originally, these papers had suggested that the local density augmentation was related to the isothermal compressibility.[6,9] One such example is shown in Figure 2 for the SCF augmented density (defined as $\rho_{local} - \rho_{bulk}$) as a function of bulk density for dilute pyrene in supercritical C_2H_4.[9] These measurements were made using steady-state fluorescence spectroscopy and examining changes in the intensity of the vibronic structure in the fluorescence spectrum of pyrene, which is solvent sensitive. Although the authors originally suggested that the augmented density was related to the isothermal compressibility,

it is clear from Figure 2 that the maximum in the local density enhancement is well below the highest isothermal compressibility, which occurs in the vicinity of the critical density.

The local density augmentations extracted from spectroscopic measurements described above depend on the spatial range of the measurement technique. The range measured by the absorption, fluorescence, and EPR probes is the distance over which those probes are influenced by the solvent. Since all of these probes are nonionic, one would expect that they would be influenced by forces that decrease as $1/r^6$. Thus, it is most likely that the distance reported by the local density probes is 1−2 solvent molecular diameters. Of course, the details of the solute/solvent interaction potential will depend on the specific nature of the compounds involved.

The local density augmentation results have been corroborated by numerous experimental studies that include UV−vis solvatochromic shifts,[10] steady-state fluorescence,[11−13] and collisional deactivation.[14] Some of these techniques are reviewed in a report by Kauffman.[15] Rotational diffusion measurements have proven to be an additional probe of local environments in SCFs.[16,17]

On the basis of their studies of the formation and fluorescence of twisted intramolecular charge transfer states of (dimethylamino)benzonitrile (DMABN) and ethyl(dimethylamino)benzoate (DMAEB) in SC CO_2, C_2H_6, and CHF_3 Fox and co-workers[11] proposed a three-region model of local density augmentation that included gas-phase solute−solvent clustering at low densities, clustering in the near-critical region and liquidlike solvation at high densities. On the basis of his own studies of the DMABN, Kajimoto and co-workers proposed a Langmuir-type adsorption model to describe the effects of local density augmentation on the probe.[18] In addition to the wealth of experimental studies, local density augmentation has been corroborated by integral equation theory calculations[19] and molecular dynamics simulations.[12,20]

B. Preferential Solvation

It is quite common to add small amounts of cosolvents to SCFs (especially CO_2) to increase the solubilities of heavy organic solutes. In such cases, the cosolvents are chosen to have size and interaction energies (e.g., Lennard-Jones parameters) intermediate between those of the SCF and the solute. As a result it is not surprising that the solute would be preferentially solvated by the cosolvent. This is shown in Figure 3 for the preferential solvation of phenol blue in SC CO_2 at 35 °C, with a variety of added cosolvents present at a bulk composition of 1 mol %.[21] At high densities the local composition is not very different from the bulk but at lower pressures, where the density is low and there is more free volume, the local composition can be as much as 10 times the bulk value. These measurements were obtained from solvatochromic shifts in pure CO_2 and CO_2/cosolvent mixtures. Yonker and Smith[22] found similar trends for CO_2/2-propanol mixtures using 2-nitroanisole as a UV−vis solvatochromic probe.

Subsequently, local compositions of cosolvents around dilute solutes as large as 10 times the bulk

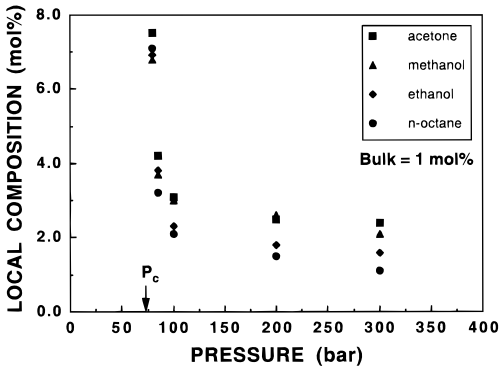

Figure 3. Local compositions of cosolvents around phenol blue in supercritical CO_2 at 35 °C determined from solvatochromic shifts (data from ref 21).

values have been measured by both absorption[23,24] and fluorescence spectroscopies.[13,25,26] Moreover, they have been corroborated by integral equation theory calculations.[13,27]

A special type of preferential solvation is the attraction of a dilute solute for itself. Solute/solute interactions and the calculation of solute/solute radial distribution functions has been an area of significant interest. Some examples of this work can be found in the work of Lee[19] and Randolph.[28]

Thus, one would expect the local density around a dissolved solute in compressed gases and SCFs to be greater than the bulk. In addition, if an attractive cosolvent (typically present at 0.5−5 mol %) is present, the local environment around the solute will be enriched with the cosolvent, with this phenomenon being much more pronounced at lower pressure where the mixture is less dense and has more free volume.

While local density augmentation and local composition enhancement can occur in liquid solutions,[29] it tends to be more pronounced in low-density supercritical fluids. In liquid solutions the density is already very high so significant local density enhancement is precluded by the high-density close-packed limit. In addition, at liquid densities, packing effects (i.e., the size of the various molecules) play a larger role in determining local compositions. In supercritical fluids the bulk density can be just $^1/_4$ or $^1/_2$ the close packed density limit. Thus, the molecules have significantly more free volume within which to arrange themselves in energetically favorable positions. Thus, it is possible that local solvation effects may have a larger effect on reaction kinetics in SCFs than might be observed in liquid solutions.

C. Thermodynamic Pressure Effect on the Rate Constant

Many reactions can be analyzed in terms of transition-state theory,[30] which assumes a reaction model in which there is a thermodynamic equilibrium between the reactants and a transition state. For a simple bimolecular reaction, this would be

$$A + B \leftrightarrow [\text{transition state}]^{\ddagger} \rightarrow \text{products}$$

From this the thermodynamic pressure effect on a bimolecular rate constant[31] can be obtained as

$$RT\left(\frac{\partial \ln k_{bm}}{\partial P}\right)_T = -\Delta\bar{v}^{\ddagger} - RT\kappa_T$$

where k_{bm} is the bimolecular rate constant (M^{-1} s^{-1}); $\Delta\bar{v}^{\ddagger}$, $\bar{v}_{TS} - \bar{v}_A - \bar{v}_B$, reaction activation volume; $\bar{v}_i$, partial molar volume of component i; κ_T, mixture isothermal compressibility; P, pressure; R, gas constant; and T, absolute temperature.

The thermodynamic pressure effect on the rate constant is simply the difference in the partial molar volumes of the transition state and the two reactants minus a compressibility term. The expression for a unimolecular reaction is similar except that the activation volume is just the difference in the partial molar volume of the transition state and the reactant and the isothermal compressibility term drops out. The thermodynamic pressure effect on reactions can be significant, dependent on the nature of the transition state and the reaction, since values of partial molar volumes of dilute solutes in SCF's can be very large, usually negative, values. In fact, experimental measurements of partial molar volumes have been reported in the literature[32] as large as $-15\,000$ cm^3/mol.

The partial molar volume of a dilute solute is proportional to the isothermal compressibility so activation volumes will be largest near the critical point of the mixture. Thus, the thermodynamic pressure effect on reaction rate constants can be much larger in SCFs than is observed in liquids due to the long-range density fluctuations that result in a large isothermal compressibility of the solvent and large partial molar volumes of dilute solutes. Examples will be given below where the activation volumes are 1000 times larger in the SCF than in liquid solutions. This means that a small change in pressure can result in a large change in the reaction rate constant. In liquids, that same change in pressure would hardly affect the reaction rate constant.

Although pressure is inevitably the experimentally controlled variable, sometimes the analysis of rate data can be facilitated by examining how the rate constant varies with solvent density:

$$\left(\frac{\partial \ln k_{bm}}{\partial P}\right)_T = \left(\frac{\partial \ln k_{bm}}{\partial \rho}\right)_T \left(\frac{\partial \rho}{\partial P}\right)_T = \frac{-\kappa_T}{V}\left(\frac{\partial \ln k_{bm}}{\partial \rho}\right)_T$$

where k_{bm}, κ_T, P, and T are as previously defined and ρ is density and V is molar volume.

This effectively factors out the large (and important) influence of the isothermal compressibility and allows more careful examination of the other influences on the reaction.

Therefore, we might anticipate that both long-range density fluctuations and short-range solvation might affect reactivity in supercritical fluid solutions. Below, we investigate how these two factors influence diffusion-controlled reactions, activated reactions, reaction equilibria, and exhibit cage effects on reactions.

III. Reactions That Probe Solvation in Supercritical Fluids

The best reactions to probe the influence of solvation are unimolecular and bimolecular ones that are solvent sensitive. Below we discuss reactions of this type, including diffusion-controlled reactions, activated reactions, equilibrium limited reactions, and reactions that might exhibit cage effects, to probe the influence of short-range solvation and long-range density fluctuations on reactivity in SCFs.

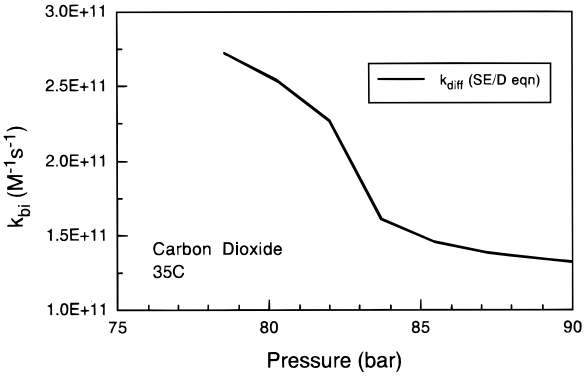

Figure 4. Expected diffusion-controlled rate constants in CO_2 at 35 °C as a function of pressure (data from ref 26).

A. Diffusion-Controlled Reactions

Reactions that are normally diffusion-controlled in liquid solutions are excellent probes of solvation in SCFs. Fully diffusion-controlled reactions would be ones in which there is no activation energy and which have a reaction probability of one; i.e., reactions in which two species react instantaneously upon collision. In particular, these types of reactions can address the question of whether increased local densities or increased local compositions in any way enhance or retard translational diffusion or the collision process.

In liquid solutions, diffusion-controlled rate constants can be modeled effectively with the Smoluchowski equation, $k_{diff} = 4\pi N\rho D$, where D is the diffusion coefficient, N is Avogadro's number, and ρ is the reaction distance. If diffusion coefficients are not available, as is frequently the case for solutes in SCFs, the Stokes−Einstein equation, that relates diffusion coefficents inversely to the solution viscosity, can be used. This yields the Stokes−Einstein-based standard Debye equation (SE/D), $k_{diff} = 8RT/3\eta$, where η is the solvent viscosity. Since viscosity is a function of density, which can be varied substantially with small changes in temperature or pressure in the near-critical region, diffusion-controlled rate constants, as predicted by the SE/D equation should decrease rapidly with increasing pressure in that region, as shown in Figure 4. At lower pressures, diffusion-controlled rate constants should equal the collision rate constants predicted by the kinetic theory of gases,[33] $k_{diff} = 4\pi(R_c)^2(T/\pi)^{0.5}$, where R_c is the collision radius and T is the absolute temperature. Randolph and co-workers[34] have investigated the transition from kinetic theory to Smoluchowski behavior using Brownian and molecular dynamics. Although the transition is dependent upon the collision radius, the Smoluchowski equation should be good down to about a reduced density of 1.0, where the gradual transition to kinetic theory behavior begins, as shown in Figure 5. Most of the experiments

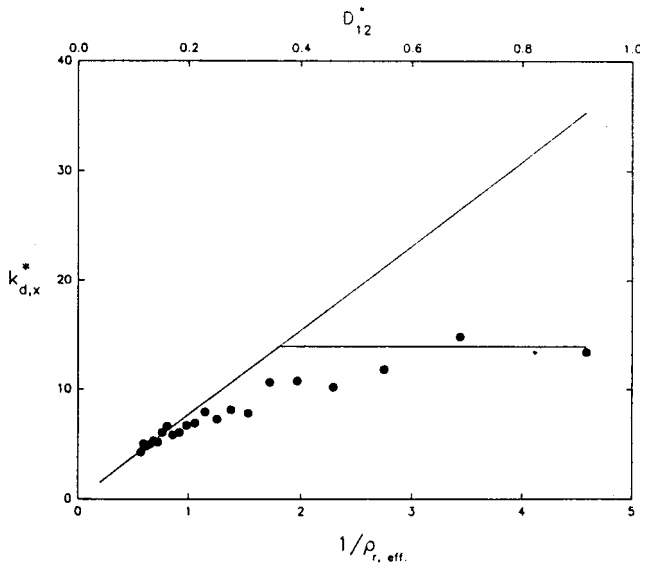

Figure 5. Reaction rate constant vs diffusion coefficient, in solute Lennard-Jones units, as determined from Brownian dynamics. The corresponding effective inverse reduced density is also shown, as well as the values from kinetic theory (horizontal line) and the Smoluchowski limit (diagonal line). (Reprinted with permission from ref 34. Copyright 1995 American Institute of Chemical Engineers.)

described below are at reduced densities greater than 1.0. Reactions that have been studied include pyrene excimer formation, spin-exchange reactions, radical recombinations and triplet/triplet annihilations, and fluorescence quenching reactions.

1. Pyrene Excimer Formation

Pyrene excimer formation is diffusion-controlled in liquids and was an excellent choice to probe local solvation effects on reaction rates in SCFs since pyrene had been used previously to measure local densities.[9,12] Bright and co-workers[35] used time-resolved fluorescence spectroscopy to measure the monomer and excimer fluorescence and fit the data to determine the rate constant for excimer formation. They reported that the rate constants for pyrene excimer formation matched those predicted from the SE/D equation in SC CO_2 and SC C_2H_4.[35] However, in SC CHF_3 and CO_2 modified with small amounts of acetonitrile or methanol, the pyrene excimer formation rates were as much as 30 times below SE/D.[35] The explanation offered at the time was that the polar SCF and polar cosolvents were more effective than the nonpolar solvents in clustering around the pyrene solute, thus impeding its motion. These studies, in particular, prompted much speculation about the nature of the local solvent environment around dissolved solutes in SCFs and its potential influence on chemical and physical processes. Subsequently, the authors have reanalyzed the original data and now find that all of the pyrene excimer formation rate constants match SE/D. This result is corroborated by a recent study of the photodimerization of anthracene in SC CO_2, which occurs at diffusion control and is not influenced by increased local densities.[36] Subsequently, there have been additional studies of pyrene in SCFs.[11d,37,38]

2. Spin-Exchange Reactions

Randolph and co-workers[39] studied the Heisenberg spin-exchange reaction between nitroxide free radicals in SC ethane using EPR spectroscopy. The actual rate constants measured were below those predicted by SE/D. However, the spin-exchange reaction is envisioned as consisting of the two radicals diffusing together but reaction only occurring with some reaction probability that depends on the exchange integral, which is a property of the radical, and the collision time. By fixing the collision time at high pressures and assuming that SE/D adequately describes the rate at which the radicals come together, it was found that the collision time (which is on the order of 10^{-14} s) must increase at lower pressures where the bulk density is relatively low (i.e., ρ_r close to 1.0, where ρ_r is the reduced density $= \rho/\rho_c$). The authors suggested that the increased local density around the radical pair might be the cause of the increased (by about a factor of 3) collision times. Since this reaction is actually well below diffusion control (0.22 SE/D at 308 K and the highest pressures studied), the results do not so much shed light on the effect of solvation on the translational component of diffusion-controlled reactions (as was being probed by the pyrene excimer formations studies above) but rather on the possibility of the increased local density influencing an encounter complex.

3. Radical Recombination and Triplet–Triplet Annihilation

In liquid solutions benzyl radicals are known to recombine at the diffusion-controlled limit, as long as a spin statistical factor, which depends only on the nature of the radical pair, is taken into account.[40] This factor takes the conservation of spin multiplicity into account. For two doublet free radicals such as benzyl radicals, there are four possible spin states for the encounter complex and only one of those four will result in formation of the bibenzyl product so the spin statistical factor is $^1/_4$. Thus, benzyl radical recombination is a clean test of solvent effects on simple diffusion-controlled reactions. Roberts et al.[41] found that benzyl radical recombination rates came within a factor of 2 of the expected $^1/_4$ SE/D limit over a wide range of pressures in both SC CO_2 and SC C_2H_6. In a companion report they found identical results for SC CHF_3 and CO_2 modified with a small amount of acetonitrile.[41] They concluded that truly diffusion-controlled reactions do, in fact, occur at the expected diffusion-controlled limit in SCFs.

The benzyl radical recombination results were corroborated by measured rates of the triplet−triplet annihilation (TTA) of benzophenone in SC CO_2, C_2H_6, CHF_3, and acetonitrile modified CO_2.[41] The spin statistical factor for this reaction is $^5/_9$ and the rate constant for benzophenone TTA in liquid solution matches $^5/_9$ SE/D quite well. Moreover, the measured values in SCFs and the CO_2/acetonitrile SCF mixture follow $^5/_9$ SE/D predictions remarkably well. An example of these results is shown in Figure 6 for SC CO_2 and CO_2/1 mol % acetonitile solutions at 35 °C.

Worrall and Wilkinson[42] report a very similar study of triplet−triplet energy transfer between anthracene and azulene and benzophenone and naphthalene in

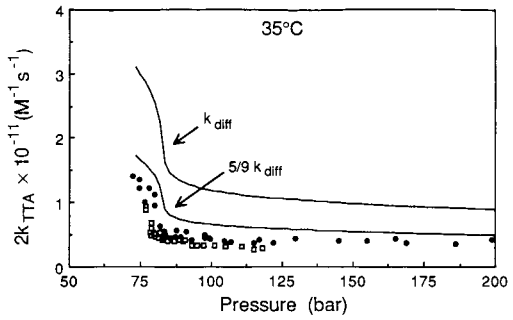

Figure 6. Plot of the pressure dependence of the triplet−triplet annihilation rate constant of benzophenone triplet in a 1 mol % CH_3CN/CO_2 mixture (□) and in pure SC CO_2 (●) at 35 °C compared to k_{diff} (see text). (Reprinted from ref 41b. Copyright 1993 American Chemical Society.)

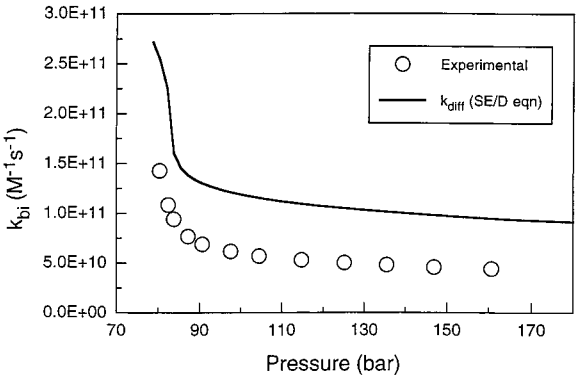

Figure 7. Plot of the pressure dependence of the bimolecular rate constants for the fluorescence quenching reaction of anthracene/CBr_4 in CO_2 at 35 °C, compared to predictions from the Stokes−Einstein-based Debye equation. (Reprinted from ref 26. Copyright 1997 American Chemical Society.)

SC CO_2 and CO_2/acetonitrile and CO_2/*n*-hexane mixtures. They report bimolecular rate constants at just one state point, 175 bar and 45 °C, but perform the experiments at acetonitrile and *n*-hexane concentrations from a couple mole percent in CO_2 all the way to 100% of the liquid. The bimolecular rate constants decrease with increasing acetonitrile or *n*-hexane concentration, in line with what one might expect for increasing bulk viscosity in CO_2/acetonitrile or CO_2/*n*-hexane mixtures. However, in no case does the reaction take place at the SE/D limit predictions. In neat liquid acetonitrile and *n*-hexane, the reactions have probabilities of energy transfer per encounter ranging from 0.36 to 0.46. In pure CO_2 this probability reaches as high as 0.84. The authors suggest an explanation similar to that presented for the Heisenberg spin-exchange reaction discussed above; i.e., that the increased local density forces a longer lifetime of the encounter complex, increasing the reaction probability per encounter. Investigations of these two reactions in pure CO_2 as a function of pressure would provide a clearer interpretation.

4. Fluorescence Quenching

Bunker and Sun[43] reported rate constants for the fluorescence quenching of 9,10-bis(phenylethynyl)-anthracene (BPEA) with carbon tetrabromide in SC CO_2. In hexane this reaction occurs at 0.34 SE/D. In SC CO_2 at high densities, the quenching rate is 0.18 SE/D. If the entire set of data are multiplied by the factor needed to make the data and SE/D match at high pressures, the low-pressure data rise above SE/D. Thus, these data show a very similar trend to the Heisenberg spin-exchange data[39] discussed above; i.e., the rate constants are below SE/D but the factor that the data fall below SE/D is smaller at lower pressures. Bunker and Sun interpret this as increased local compositions of the carbon tetrabromide influencing a diffusion-controlled reaction. However, for a true diffusion-controlled reaction, the two species react as soon as they come in contact. Thus, it is not possible for an increased local concentration of one of the reactants to build up around the other. We believe there are two other possible explanations for the trends measured for the quenching of BPEA with carbon tetrabromide. One is that, like the spin-exchange reaction, this reaction might be one characterized by the two species diffusing together and then having some probability of actually reacting dependent on the contact time. The increased density of the solvent around the encounter complex at lower pressures could be increasing the contact time once the reactants diffuse together and, thus, may result in a higher reaction probability. Alternatively, the reaction may have a small activation barrier and, if that is the case, it is quite possible that it could be influenced by the local composition of the carbon tetrabromide around the BPEA, as discussed for similar systems below.

Zhang et al.[26] have reported on the kinetics of two energy-transfer reactions measured by fluorescence quenching that do occur at the SE/D limit in liquids: anthracene/CBr_4 and 1,2-benzanthracene/CBr_4. The bimolecular rate constants for the anthracene/CBr_4 reaction in CO_2 at 35 °C are shown in Figure 7, where they are compared to the SE/D predictions. The data follow the trend of SE/D very well but consistently fall about a factor of 2 below SE/D. The authors conclude that the measured values are at the diffusion-controlled limit since it is well-known that the Stokes−Einstein equation overpredicts diffusion coefficients in SCFs by as much as 100%.[44] Of course, the reason that SE overpredicts diffusion coefficients in SCFs is an unanswered question of considerable interest. In contrast, SE/D predictions of diffusion-controlled rate constants in liquids are generally quite good.

Subsequently, Sun and co-workers[45] have also measured fluorescence quenching of the anthracene/CBr_4 system, as well as perylene with CBr_4, and found both reactions to follow the trend of SE/D when multiplied by a factor of 4−5. 9,10-diphenylanthracene/CBr_4 and 9-cyanoanthracne/CBr_4 were a factor of about 4 and 12 below SE/D but the discrepancy was slightly less at the lower pressures (like the BPEA/CBr_4 system above). As before, the authors attributed this to local composition enhancements of a diffusion-controlled reaction but, as discussed above for BPEA/CBr_4, there may be other explanations.[26]

In summary, the studies of the kinetics of various diffusion-controlled and near-diffusion-controlled re-

Scheme 1

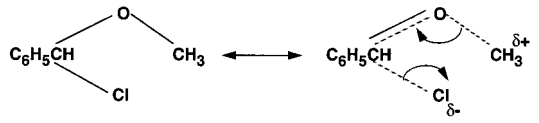

actions in SCFs described above support two general conclusions. First, reactions that involve reaction as soon as the diffusing reactants come in contact occur at the expected diffusion-controlled limit in SCFs. Except for the unexplained overprediction of diffusion coefficients by SE, translational diffusion is not enhanced or impeded by increased local densities or local compositions. Second, reactions that are somewhat below SE/D in liquids and are envisioned as occurring by the two reactants diffusing together and then experiencing some probability that the encounter complex will result in the formation of products can be enhanced by the increased local density providing for greater contact time for the encounter pair.

B. Kinetically-Controlled Reactions

Activated reaction processes have the potential to be influenced by long-range density fluctuations, which result in large partial molar volumes, as well as short-range local density and local composition effects.

1. Activation Volumes

As described above, the rate constants for reactions can vary dramatically with pressure if the transition state and the reactants are sufficiently different. If this is the case, the reactants and the transition state will have very different partial molar volumes. This might occur if nonpolar reactants proceed through a polar transition state, in which case one would expect the partial molar volume of the transition state to be a larger negative value. For a unimolecular process, $RT(\partial \ln k/\partial P)_T = -\Delta\bar{v}^{\ddagger} = -(\bar{v}_{TS} - \bar{v}_R)$. If $\bar{v}_{TS}$ is a larger negative value than $\bar{v}_R$, then one would expect the rate constant to increase with increasing pressure. This is exactly what was observed by Johnston and Haynes[46] for the thermal unimolecular decomposition of α-chlorobenzyl methyl ether in supercritical 1,1-difluoroethane. The decomposition, $C_6H_5CHCl-O-CH_3 \rightarrow C_6H_5CHO + CH_3Cl$, is believed to proceed by an E1 mechanism through a polar transition state as shown in Scheme 1.

Johnston and Haynes[46] experimentally measured activation volumes as large as −6000 cm^3/mol. This resulted in unimolecular rate constants that changed by over an order of magnitude with a 10−15 bar increase in pressure, as shown in Figure 8. The authors found that the pressure effect on the reaction rate constant was better described by an expression for the free energy of transferring a dipole from a vacuum into a delectric medium when local dielectric constants (i.e., local densities) were used.

Diels−Alder reactions are also ideal bimolecular reactions to probe the effect of long-range density fluctuations in supercritical fluids, as manifested through the activation volume. They involve the

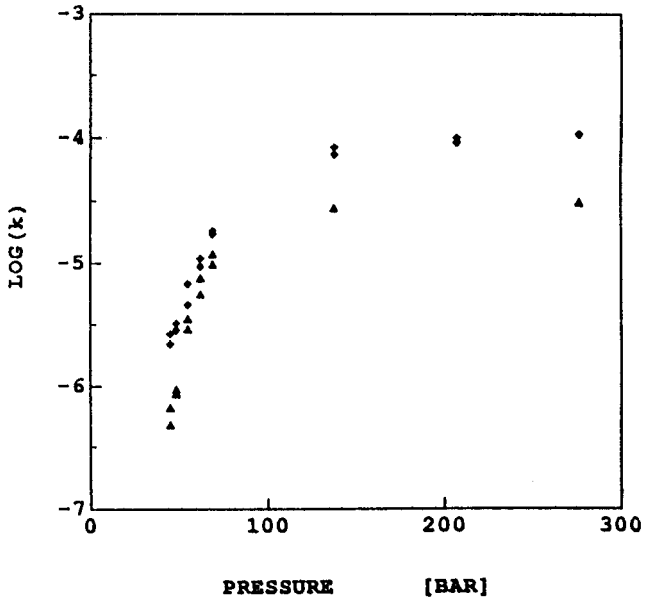

Figure 8. Rate constant for the unimolecular decomposition of α-chlorobenzyl methyl ether in supercritical 1,1-difluoroethane at 403 K (▲) and 423 K (♦). (Reprinted with permission from ref 46. Copyright 1987 American Institute of Chemical Engineers.)

Scheme 2

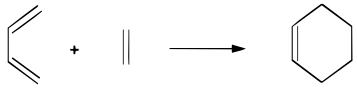

addition of an alkene or alkyne to a diene, as shown in Scheme 2 for butadiene reacting with ethylene to form cyclohexene.

Besides being of considerable commercial interest, Diels−Alder reactions are clean, well-characterized reactions that generally proceed in a single step through a pseudo-aromatic transition state. The mechanism is the same in the gas and liquid phases. Paulaitis and Alexander[47] measured the rate of the Diels−Alder cycloaddition of maleic anhydride with isoprene in supercritical CO_2. The rate constants increased with increasing pressure at all temperatures, with the most dramatic effect at 35 °C and pressures close to the critical point. This is expected since it is in this region that the isothermal compressibility and, subsequently, the reactant and transition state partial molar volumes, are largest in magnitude. Paulaitis and Alexander[47] also point out that the activation volume will only exhibit a strong divergence at the critical point for dilute solutions; i.e., finite concentrations of solute will diminish the effect. Other researchers have also measured large activation volumes for Diels−Alder reactions in SCFs.[48] In some cases, attempts were made to correlate the rate constants with solvatochromic shifts. However, as described above, solvatochromic shifts measure the local solvation, whereas in dilute solution the activation volume is proportional to the isothermal compressibility, which is a long-range effect. It is certainly true that at pressures above the critical pressure the larger local density augmentations and local composition enhancements coincide with high compressibility but this is not true

at pressures below the critical pressure (as seen in Figures 1 and 2). The solvatochromic shifts are measuring local solvation and the isothermal compressibility is a measure of long-range density fluctuations. Thus, one would not expect solvatochromic shifts and the rate constants of dilute Diels−Alder reactions to correlate very well over wide ranges of pressures or densities that include subcritical regions. It should be noted that the selectivity results of Ikushima et al.[48a,b] are suspect since Renslo et al.[49] have subsequently shown that some of those experiments were performed in the two-phase region, with only a portion the reaction volume sampled for analysis.

The rates of reactions involving ionic species are likely to be very sensitive to pressure in SCFs. This is due to the electrostriction of the solvent around the ions that can result in large negative partial molar volumes. Moreover, the magnitude of the partial molar volume strongly depends on the size of the ion. The pressure effect on ionic reactions in SCFs has been demonstrated by Zhang et al.[50a] who measured the rates of arylmethyl cation ion−neutral reactivity in SC CHF_3 and C_2H_6. Specifically, they used pulse radiolysis to investigate the reaction of benzhydryl cation (Ph_2C^+H) with tetramethylethylene (TME) in CHF_3 at 35 and 50 °C, and with triethylamine (TEA) in CHF_3 at 35 and 70 °C. Also, they measured the rates of the 4,4-dimethoxybenzhydryl cation ($(4\text{-}MeOPh)_2C^+H$) with TEA in CHF_3 at 35 and 70 °C, and with TEA in C_2H_6 at 35 °C. In all cases, the ionic product (and transition state) were larger than the reactant ion and, therefore, were better able to delocalize the charge. Thus, the rates were fastest at low pressures, where the solvent density and dielectric constants are low. The measured activation volumes were as large as -1700 cm^3/mol at 35 °C in CHF_3. Moreover, the activation volumes could be adequately described by either the Drude−Nernst equation or the compressible electrostriction model developed by Wood and co-workers.[50b] Although there were some indications of preferential solvation (vide infra), the main influence on these reactions was the pressure effect on the rate constants caused by the electrostriction of the solvent around the different sized ionic species. Although supercritical water is not included in this review, electrostriction is particularly important for reactions in that medium.[51]

2. Influence of Local Density

Discerning the influence of local density augmentation or local composition enhancements on reaction rates is much more challenging than measuring the overall activation volume, which in many cases may be the predominant pressure effect on the reaction rate. Nonetheless, there have been a number of studies in which either the thermodynamic pressure effect on the rate constant is expected to be small, it can be reasonably estimated or the local solvation influence on the reaction rate can be differentiated from the general expected trend of the thermodynamic pressure effect on the reaction.

One such case is the rate of intramolecular charge-transfer state formation for 4-(*N*,*N*-dimethylamino)-benzonitrile (DMABN) in supercritical CHF_3. The steady-state intensities of the locally excited and charge-transfer bands of this compound have served as excellent probes of local density.[11,18] Kajimoto and co-workers[52] expected that the rate of the charge transfer state formation would increase with increasing density and this is what was observed experimentally. As shown in Figure 9, the logarithm of the rate constant is relatively linear with bulk solvent density, except in the low-density region between about 0.15 and 0.35 g/cm^3, where the rates are higher than expected based on bulk density. The authors attribute this to the increased local density of the CHF_3 solvent around the DMABN, which increases the local dielectric constant, which in turn promotes the rate at which the charge-transfer complex is formed. They use molecular dynamics simulations to determine the number of CHF_3 solvents clustered in the local environment around the DMABN. In addition, they point to the continued increase in the rate at higher densities as evidence that the increased local density is promoting the reaction by lowering the activation barrier for the charge transfer, as well. Thus, there is evidence that local density enhancement can enhance reactions by both providing a denser, higher dielectric environment and stabilizing and lowering the barrier of the transition state.

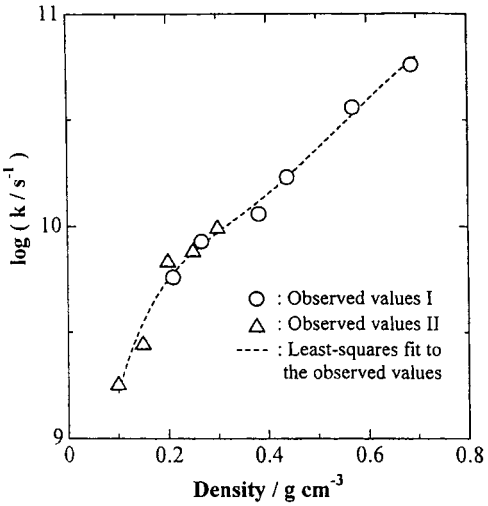

Figure 9. The density dependence of the charge transfer state formation rate for 4-(*N*,*N*-dimethylamino)benzonitrile (DMABN) at 306 nm (I) and at 274 nm (II) in supercritical CHF_3 at 50 °C. (Reprinted with permission from ref 52a. Copyright 1997 VCH Verlagsgesellschaft mbH.)

3. Influence of Local Composition Enhancement

Roberts et al.[24,27] have probed the effect of local composition enhancement by studying the reaction of a dilute species benzophenone triplet, with various reactants (quenchers) that are still dilute but present in much higher concentrations than the benzophenone. Two of the quenchers, 2-propanol and 1,4-cyclohexadiene, should be preferentially attracted to benzophenone but a third, oxygen, should not. They investigated the effect of preferential solvation by (1) measuring the reaction rates and comparing with estimates of the thermodynamics pressure effect on the reaction and (2) comparing the rates of reaction

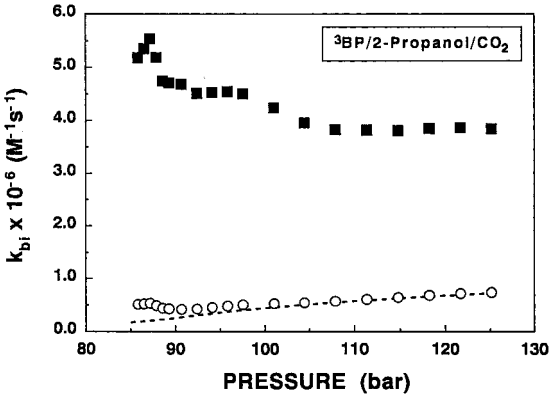

Figure 10. Experimental bimolecular rate constants for the reaction of benzophenone triplet with 2-propanol in supercritical CO_2 at 44.4 °C: (■) rate constants based on *bulk* 2-propanol concentrations; (○) rate constants based on *local* 2-propanol concentrations. The dashed line are estimates of the thermodynamic pressure effect on this reaction from the Peng−Robinson equation of state. (Reprinted with permission from ref 24. Copyright 1995 American Institute of Chemical Engineers.)

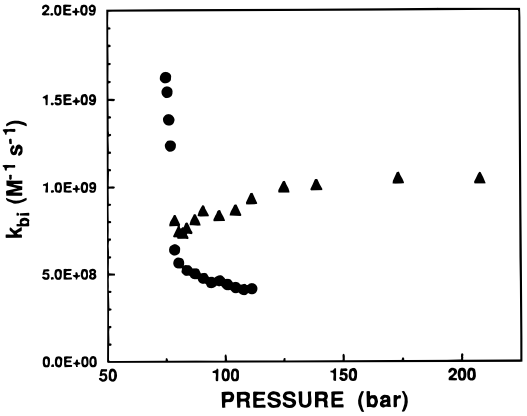

Figure 11. Comparison of the pressure dependence of the bimolecular rate constants (based on bulk concentrations) for the reaction of benzophenone triplet with 1,4-cyclohexadiene (●) and oxygen (▲) at 35 °C in CO_2. (Reprinted from ref 27. Copyright 1995 American Chemical Society.)

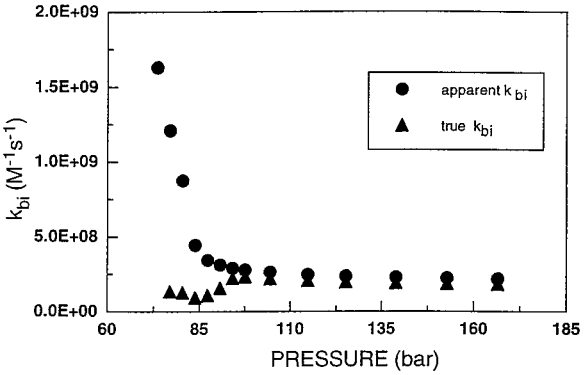

Figure 12. Bimolecular rate constants plotted vs pressure for the quenching reaction of anthracene with C_2H_5Br in CO_2 at 35 °C: (●) rate constants based on the *bulk* concentrations of the reactions; (▲) rate constants based on the *local* concentration of the C_2H_5Br around the anthracene. (Reprinted from ref 26. Copyright 1997 American Chemical Society.)

of benzophenone triplet with a preferred coreactant, 1,4-cyclohexadiene, with the rates with a nonpreferred or excluded coreactant, oxygen. While increased coreactant concentration might have a small effect on the benzophenone partial molar volume, the investigators anticipated that the most significant way that preferential solvation might influence reaction rates was through the effective concentration of one species around the other being higher than the bulk value. Thus, the reaction rate might be expressed as rate = $k_{bi}^{bulk}[^3BP][quencher]^{bulk}$ or rate = $k_{bi}^{local}[^3BP][quencher]^{local}$, where $[quencher]^{local}$ would be the local concentration of the 2-propanol, cyclohexadiene, or oxygen around the ^3BP. Figure 10 shows the rate constants for the quenching of ^3BP with 2-propanol in SC CO_2 at 44.4 °C, analyzed using both the bulk concentration of the 2-propanol and the local concentration of the 2-propanol around the ^3BP, as estimated from solvatochromic shift measurements. Also shown in the figure is an estimation of the expected pressure effect on the rate constant, calculated from Peng−Robinson equation, which agrees with the data when the local concentrations of the 2-propanol are used. In addition, Figure 11 shows the rate constants for the reaction of ^3BP with 1,4-cyclohexadiene and with oxygen, both based on the bulk concentrations. For both reactions, the estimates of the activation volume are small, suggesting very slight increases in the rate constants with increasing pressure. The apparent increase in the rate constant for the reaction with cyclohexadiene is likely due to its increased local concentration around the ^3BP. Thus, by comparing the measured reaction rates as a function of pressure and comparing them with the expected pressure effect on the rate constants, Roberts et al.[24,27] have been able to probe the influence of preferential solvation and show how it can enhance reaction rates.

Prefential solvation has also been probed with the fluorescence quenching of anthracene by bromoethane in SC CO_2.[26] Unlike the energy-transfer reactions described above in the section on diffusion-controlled reactions, this reaction has a clear activation barrier. This reaction was chosen as a probe because it is entirely solvent insensitive in liquid solutions. It occurs at a rate of 2×10^8 M^{-1} s^{-1} whether it is in cyclohexane, hexane, or acetonitrile. Unlike the Diels−Alder and other reactions discussed above that were chosen because they were expected to yield large solvent effects, this reaction was chosen because it is devoid of solvent effects. In this way, the authors were able to isolate the effect of local solvation, specifically local composition enhancement effects. The bimolecular rate constants for this reaction are shown in Figure 12. The rate constants based on the bulk concentration of bromoethane are very solvent sensitive, increasing dramatically at lower pressures. Conversely, the rate constants based on the local concentration of bromoethane around anthracene (as measured by solvatochromic shifts using that exact system) are relatively insensitive to pressure, which is more in line with expectations. This provides a strong indication that kinetically-controlled reactions can be enhanced by the preferential solvation of one component by the other. There are a number of other experimental studies that corroborate these findings.[23,53] The study by Rhodes and

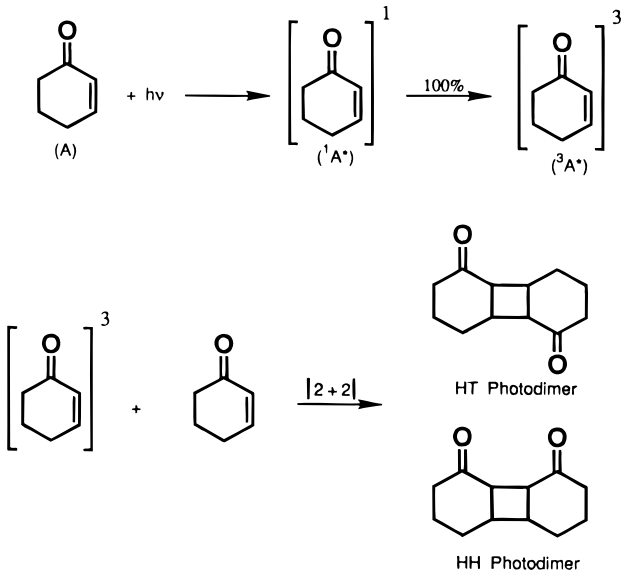

Figure 13. Photochemistry of 2-cyclohexen-1-one (A) dimerization. (Reprinted from ref 54. Copyright 1992 American Chemical Society.)

co-workers[53] is particularly interesting because it shows the influence of both local density and local composition enhancements on the Michael addition reaction of piperidine to methyl propiolate. In fluoroform, the reaction rate increases at higher densities by dielectric stabilization of the highly polar zwitterionic intermediate. However, as pressure is decreased the rate reaches a minimum and increases at lower pressures, which is attributed to local density enhancements. In addition, deviations from purely bimolecular kinetics in both supercritical fluoroform and ethane indicates the influence of increased local cosolvent concentrations (where the cosolvent happens to be the solute).

Tunable SCF solvation may also be used to influence reaction regioselectivity and stereoselectivity. Combes et al.[54] have reported on the use of SCFs to influence the regioselectivity of the photodimerization ([2+2] cycloaddition) of 2-cyclohexen-1-one. The reaction presented in Figure 13 is the reaction of the photolytically excited triplet state 2-cyclohexen-1-one with a ground-state molecule of 2-cyclohexen-1-one. The photodimer may be formed in either the head-to-tail (HT) or the head-to-head (HH) configuration. In liquid solvents the regioselectivity of HH to HT cyclohexenone dimers increases with solvent polarity. Experiments were performed in SC ethane, over the relatively small range of solvent dielectric constant from 1.3 to 1.6. The experiment showed that the regioselectivity ratio (HH/HT) actually decreased with increased solvent density, and corresponding dielectric constant. The regioselectivity changed little from 250 to 65 bar, and then, as shown in Figure 14, increased sharply at lower pressures, where the compressible region of the fluid is approached. As for the deviations of the Michael addition reaction from purely bimolecular kinetics described above, the authors explained this result in terms of enhanced solute−solute interaction, i.e., solute−solute clustering. Even though the bulk solvent density and dielectric constant is lower at lower pressures, the

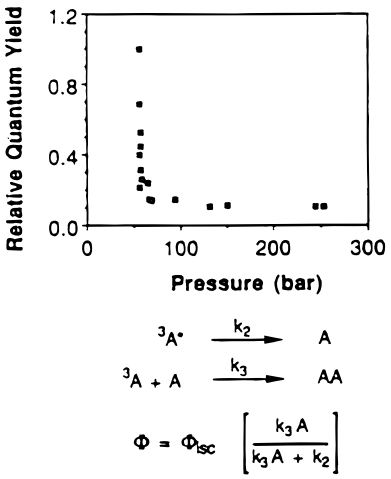

Figure 14. Relative quantum yields for cyclohexenone dimerization in SCF ethane at 35 °C and 29 mM cyclohexenone. (Reprinted from ref 54. Copyright 1992 American Chemical Society.)

increased concentration of other solutes could increase the local dielectric constant, leading to a higher HH/HT ratio. Since the excited-state triplet in this experiment is many times less concentrated than the ground-state reactant, the kinetics for this reaction are actually pseudo-first-order. Therefore, one may also view the influence on this reaction as enhanced solute−cosolute, or solute−cosolvent, since the two reacting species are so dissimilar in concentration. Stereoselectivity was also observed for the HT dimerization. The HT anti/HT syn photodimer increased from ca. 3.3−7.7 from a solvent density of ca. 2.8−4.2 g/cm^3. An identical trend was also observed in the stereoselectivity for the HT anti/syn ratio for the HT photodimers of isophorone.[55] Two explanations were offered for these observations. "The transition state leading to the HT syn configuration requires greater 'desolvation' of nearest neighbor solvent molecules. Also, it has a smaller solvent accessible area and thus occupies more volume in solution. This desolvation is understandably inhibited at higher fluid densities, hence the increased selectivity of the HT anti steroconfiguration." The ability to influence reaction regioselectivity and steroselectiviy opens exciting avenues for SCFs as reaction media.

Activated bimolecular reactions involve many collisions of the two species before an encounter occurs that can surmount the activation barrier. Thus, unlike true diffusion-controlled reactions, an equilibrium distribution of components will exist. Since the time scale for reaction is very long compared to the solvation process and the solvent dynamics, if affected one would expect the reactions to be influenced by the long time-averaged local density or local composition. The studies discussed above that have been designed to probe this solvation bear this out.

C. Equilibrium Reactions

The investigation of reaction equilibria has been an important area of study in understanding SCF solvent and solvation effects on chemical processes in sub- and supercritical fluids. These studies have

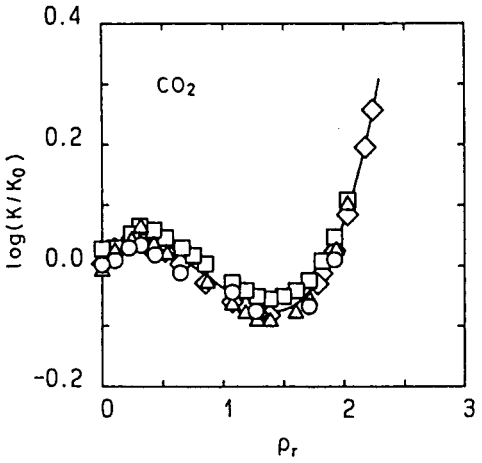

Figure 15. Equilibrium constant for 2-methyl-2-nitrosopropane dimerization in CO_2 at 60.0 °C as a function of reduced density. (Reprinted from ref 56b. Copyright 1992 American Chemical Society.)

revealed insights on how SCF solvent dynamics, and "pressure tuning" may influence, or direct the outcome of chemical reactions carried out in SCF media. These studies include intermolecular equilibria, intramolecular equilibria, and equilibria between solute and SCF.

1. 2-Methyl-2-nitrosopropane Dimer

One of the first studies of how SCFs influence chemical equilibria was the investigations of Kimura et al.[56,57] These investigators studied the dimerization of 2-methyl-2-nitrosopropane from gas to liquid densities in CO_2, CHF_3, $CClF_3$, Ar, and Ne. These investigators determined the dissociation rate constants for 2-methyl-2-nitrosopropane dimer by the stopped-agitation method in low solvent density regions, and by the density (pressure) jump method in high solvent density regions. The equilibrium constants reported for this reaction varied dramatically from low, subcritical densities to high SCF densities. Figure 15 presents the equilibrium constant for 2-methyl-2-nitrosopropane dimerization versus reduced density of CO_2. The authors invoked a three density SCF regime to explain their results. The equilibrium constant for dimerization (K_c) increased with density in the low-density regime, $\rho_r < 0.3$, and then K_c decreased with solvent density in the medium-density regime, $0.3 < \rho_r < 1.4$, and then increased again with increasing density in the high-density regime, $\rho_r > 1.4$. The authors argued that the results in the high-density regime are similar to those observed in liquid CCl_4[57] and are dominated by packing effects, whereas attractive intermolecular forces and solute−solvent interactions are important in the low-density regime, with solvent−solvent and multibody interactions becoming important in the medium-density regime.

2. Hydrogen Bonding

There have been several investigations of the chemical equilibria involved in hydrogen bonding. These studies are closely related to investigations of tautomeric equilibria described below.

In 1991, Fulton and co-workers[58] reported the use of FTIR spectroscopy to measure the degree of intermolecular hydrogen bonding between molecules of methyl alcohol-*d* (MeOD) in SC ethane and CO_2. It was determined that an equilibrium is established between free non-hydrogen-bonded monomer and hydrogen-bonded oligomers, and that fluid pressure, temperature, and alcohol concentration significantly affect the equilibrium. Both sub- and supercritical binary solutions containing up to 0.07 mol fraction MeOD under pressures and temperatures ranging from 30 to 400 bar and 40 to 80 °C, respectively, were investigated. The onset of hydrogen bonding in SC ethane occurred at 0.003 mol fraction MeOD and became extensive at 0.05 where the tetramer is believed to be the dominant species. In SC CO_2, the onset occurred at higher concentrations (mole fraction of 0.005) than expected. This, combined with additional spectral data indicated that a weak interaction between alcohol monomer and the CO_2 solvent exists. Kazarian et al.[59] have also used FTIR to study the effects of solvent density on the hydrogen bonding between perfluoro-*tert*-butyl alcohol (PFTB) and dimethyl ether (DME) in SC SF_6 as solvent. These investigators chose strongly interacting pairs of reactants, both of which had appreciable vapor pressures. This allowed, for the first time, hydrogen-bonding equilibria measurements from the gas phase, i.e., no solvent, to liquidlike densities in a SCF solvent. A modified lattice fluid hydrogen-bonding (LFHB) model was used to calculate the effects of density on free PFTB and determine K_c. The authors unequivocally demonstrated that increased density caused an increase in free PFTB with a concomitant decrease in the concentration of the PFTB/DME hydrogen-bonded complex. Also, an isothermal dependence on K_c was observed with some evidence of enhanced solute−solute interactions occurring in the compressible region of the fluid. Gupta et al.[60] reported similar results for the hydrogen bonding between methanol and triethylamine in SF_6, and found that the free energy of hydrogen bonding is stabilized by a decrease in density, i.e., the donor and acceptor are destabilized more than the complex as the solvation is reduced. In related work, Meredith et al.[61] have used FTIR spectroscopy to measure equilibrium constants for the electron donor−acceptor interactions of CO_2 with three Lewis bases: triethylamine (TEA), pyridine (PYR), and tributyl phosphate (TBP). The average K_c values determined in liquid pentane solvent at 25 °C were 0.046 (CO_2−TEA), 0.133 (CO_2−PYR), and 1.29 (CO_2−TBP). The lattice fluid hydrogen-bonding model was used with the spectroscopically determined K_c values to predict bubble points for the CO_2−TEA and CO_2−TBP systems. The calculations revealed that the relatively weak specific interactions will have a measurable effect on phase behavior.

3. Tautomeric Equilibria

In 1989, Johnston and co-workers[62] reported SCF solvent effects on the tautomeric equilibria of 2-hydroxypyridine and 2-pyridone at near infinite dilution. The SC fluids used were propane at 393 K and 1,1-difluoroethane at 403 K, and the pressure ranged

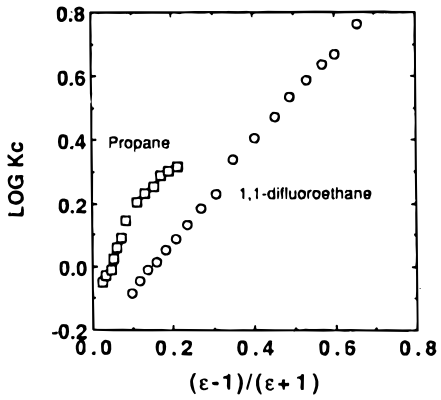

Figure 16. Kirkwood model for solvent polarity effect on K_c for the tautomerization of 2-hydroxypyridine/2-pyridone in supercritical 1,1-difluoroethane at 403 K (○) and in supercritical propane at 393 K (□). (Reprinted from ref 62. Copyright 1989 American Chemical Society.)

from 21 to 206 bar. The equilibrium constant, K_c, was measured by in situ UV spectroscopy and was found to increase 4-fold for a pressure increase of 40 bar in 1,1-difluoroethane, with a corresponding change in partial molar volume reported to be -1400 cm^3/mol. Since the tautomers of the equilibrium were of comparable size, it was suggested that the effect of pressure on their equilibrium should reflect the difference in the tautomers polarity. Therefore, the results were analyzed in terms of Kirkwood theory that may be used to describe the relationship between K_c and solvent polarity, according to

$$RT \ln K_c = \frac{3}{8}\left(\frac{1-\epsilon}{1+\epsilon}\right)\left(\frac{\mu_2^2}{r_2^3} - \frac{\mu_3^2}{r_3^3}\right)$$

where ϵ is the dielectric constant, r is the molecular radius, μ is the dipole moment, and subscripts 2 and 3 refer to the two tautomers. Figure 16 presents log K_c versus the Kirkwood solvent parameter, for the tautomeric equilibria of 2-hydroxypyridine and 2-pyridone in the two SCF solvents investigated. The results demonstrated that as the solvent polarity increased, K_c increased favoring 2-pyridone, the more polar tautomer. The authors noted that at any given value of ϵ, K_c is larger in propane than in 1,1-difluoroethane, and it was suggested that this may be explained by the larger value of polarizability per volume of propane at a given value of ϵ.

Tautomeric equilibria involving β-diketones, and specifically the keto−enol tautomerization of 2,4-pentanedione has been of considerable interest due to their potential use to solublize metals as metal chelates in SCFs. In 1991, two NMR studies reported conflicting results regarding the tautomeric equilibria of 2,4-pentanedione in CHF_3. Yamasaki and Kajimoto[63] reported that the tautomeric equilibrium constant was almost independent of CHF_3 solvent density, whereas Akao and Yoshimura reported that the tautomeric equilibrium in CHF_3 was shifted to the keto form as density was increased. Akao and Yoshimura[64] also observed that $K_{(keto-enol)}$ demonstrated no anomalies near the critical density of the solvent. In 1993, Yagi et al.[65] reported the results of an FTIR investigation of the solvent density dependence of tautomerization of 2,4-pentanedione in SC CO_2. In addition to addressing the previously stated literature conflict, SC CO_2 was chosen as the solvent to eliminate participation of the solvent as a hydrogen atom donor. Under these conditions, the intermolecular hydrogen bonding of the tautomerization could be isolated. Yagi et al. found the tautomeric equilibrium could be shifted by varying solvent density and the more polar keto form was favored at higher CO_2 density. In turn, the less polar enol form was favored at low solvent density. Also similar to the results of Akao and Yoshimura,[64] no anomalies were observed close to the critical density of the fluid. As expected, the tautomeric equilibrium was shifted to the enol in CO_2 compared to the more polar CHF_3 solvent.

O'Shea et al.[66] have investigated the azo−hydrozone tautomeric equilibrium of 4-(phenylazo)-1-naphthol in various liquid and SCF solvents. The less polar azo tautomer ($\mu = 1.79$ D) was dominant in the dilute gas phase, compressed ethane, and liquid alkanes. The equilibrium shifted to the more polar hydrozone ($\mu = 5.03$ D) in liquid and SC CO_2 to yield similar amounts of the tautomers. The shift was attributed to the Lewis acidity and large quadrupole moment of CO_2. The hydrozone tautomer being found to be >90% in CHF_3 was attributed to the solvent's large dipole moment and its ability to act as a hydrogen-bond donor.

Tomasko et al.[67] have described experiments designed to tailor SCFs using polar cosolvents (water and alcohols) to probe hydrogen-bonding networks in a variety of SCFs. In the presence of hydrogen-bonding networks, excited-state naphthols are known to proton transfer to the solvent to form naphtholate anion. Since naphtholate anions have characteristic emission spectra, steady-state fluorescence investigation of 2-naphthol and 5-cyano-2-naphthol were carried out in CO_2, ethylene and CHF_3 using water as a cosolvent, and in CO_2 using methanol as a cosolvent. However, anion was not detected under any of the experimental conditions. This indicated the lack of sufficient cosolvent structure to support proton transfer in these SCF mixtures. The authors also unsuccessfully attempted to measure the double proton-transfer reaction between methanol or ethanol and 7-azaindole to form tautomeric azaindole. The authors suggest that their results demonstrate the dynamic nature of these solutions and that SCF mixtures have a much greater free volume than do liquids at comparable densities. It was also suggested that the results are consistent with hydrogen bonding being less influential in SCFs than in liquids; however, this could be due to either less hydrogen bonding, or due to the nature of the hydrogen bonding being different in SCFs compared to normal liquids.

Eckert and co-workers[68] have recently chosen the keto−enol equilibrium of the Schiff base, 4-(methoxy)-1-(*N*-phenylforminidoyl)-2-naphthol, to demonstrate that selective cosolvents offer a sensitive tool to tailor chemical equilibria. Small amounts of certain protic cosolvents were found to shift significantly the equilibrium. The equilibrium was tuned essentially from one tautomer to the other by modifying

pure SC ethane with less than 2 mol % hexafluoro-2-propanol. The K_c was found to be a function of cosolvent concentration and mixture density, and evidence of local composition enhancement of cosolvent around the Schiff base was observed in the near-critical region. Solvent density, as well as degree of hydrogen bonding was used to tune the position of the tautomeric equilibrium. Since hydrogen bonding favors the keto tautomer, and the equilibrium constant for hydrogen bonding decreases with an increase in pressure,[60,61] an increase in pressure could be used to reduce the concentration of the keto form and result in a decrease in K_c.

Another subclass of reactions that can be used to probe local environments and that are frequently equilibrium-limited are isomerizations. By studying the isomerization of 4-(diethylamino)-4′-nitroazobenzene in SC CO_2 and comparing to results in liquid solvents, Sigman and Leffler[69] were able to show that this reaction can proceed through either an inversion or a rotation mechanism, dependent on the solvent. In an early study Aida and Squires[70] found that the rate of *trans*-stilbene isomerization and the cis/trans ratio in SC CO_2 were strongly dependent on pressure but could be adequately described by the bulk solvent viscosity; i.e., the rate is faster at conditions where the viscosity is lower. Subsequently, Nikowa et al.[71] used femtosecond spectroscopy to investigate the photoisomerization of *cis*-stilbene to the trans isomer in compressed solvent and have also found an expected inverse viscosity dependence on the rate of isomerization. Hara et al.[72] have also examined the excited-state isomerization of 2-vinylanthracene in compressed liquids and SCFs and have analyzed their results in terms of Kramers turnover. Additional studies of isomerizations, especially in light of more recent investigations of local density augmentation, local composition enhancement, and rotational diffusion in SCFs, may be of interest.

D. SCF Solvent Cage Effects

The existence of attractive solvent−solute interaction that may result in local density augmentation, "solvent clustering", raises the question of the importance of SCF solvent cage effects on reactions under sub- and supercritical conditions. In addressing this question it is important to realize that in all liquid and fluid solvents, solvent cages about solutes, and reactant pairs, will exist. This was already mentioned earlier in connection with the Heisenberg spin-exchange reaction.[8] Therefore some form of conventional solvent cage effects should be expected and may be observed, depending on the details of the particular chemical event. The question that, perhaps, is more relevant to SCF solvent dynamics is: At any given SCF density or viscosity, do SCFs exhibit extraordinary cage effects due to local density augmentation? Photochemistry and in situ spectroscopy of photolytically generated geminate radical pairs has been especially useful in the investigation of cage effects in SCFs. As in normal liquids, the observation of a cage effect on a chemical process will depend on the time scale of the chemical process in relationship to the integrity of the solvent cage.

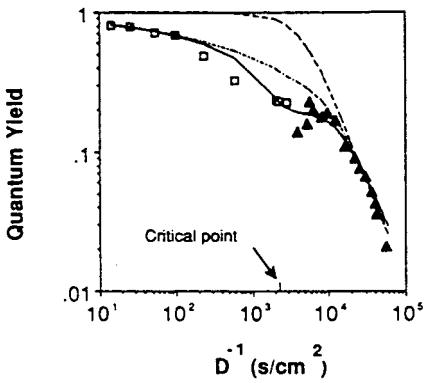

Figure 17. Quantum yield for the laser pulse photolysis of iodine in ethane at gaseous, supercritical fluid, and liquid densities. (Reprinted from ref 54. Copyright 1992 American Chemical Society.)

Molecular dynamics (MD) simulations of Petsche and Debenedetti[20] have predicted SC solvent clustering to be a very dynamic process with frequency of exchange of cluster members with the bulk to be on the order of a picosecond. More recently O'Brien et al.[73] have reported that clusters may persist for 100 ps. We shall begin our cage effect section with the classic halogen dissociation in the gas to liquid transition.

1. Quantum Yields of Iodine Photolysis

Franck and Rabinowitch[74] first proposed that a solvent cage may influence chemical reactivity in their seminal presentation of iodine atom pair recombination. The quantum yield for molecular iodine (I_2) dissociation of an isolated gas molecule is unity. However, in the presence of solvent, the dissociating iodine atom may rapidly lose excess kinetic energy through collision with the surrounding solvent and result in an in-cage recombination of the geminate pair.

$$I{-}I \rightarrow I^{\bullet} + {}^{\bullet}I$$

(gas-phase isolated molecule, $\Phi = 1$)

$$I{-}I \leftrightarrow \underset{\text{[solvent cage]}}{[I^{\bullet} + {}^{\bullet}I]} \rightarrow \underset{\text{cage escape}}{I^{\bullet} + {}^{\bullet}I}$$

Interestingly, solvent involvement is found to influence quantum yields at gas-phase densities well below the gas-to-liquid transition. Otto, Schroeder, and Troe[75] have investigated the photolytic cleavage and recombination dynamics of molecular halides in a variety of compressed bath gases (e.g., He, Ar, N_2, CO_2, C_2H_6, SF_6) over very large, gas-to-liquid, density ranges. Diffusion-based models were developed to describe the static and dynamic influences of environment on the quantum yield of I_2 photolysis in ethane as a function of the reciprocal of diffusivity. Figure 17 presents their gas (open symbols) and liquid (closed symbols) phase data, along with fits of the data. The dashed line is a fit[75] based on diffusivities. Identification of the critical point in Figure 17 demonstrates that gas-phase quantum yields are well below that expected by simple theory. The interrupted dashed line[75] invokes "a cluster effect" in terms of formation of 1:1 $I_2 + M = I_2M$ equilibrium

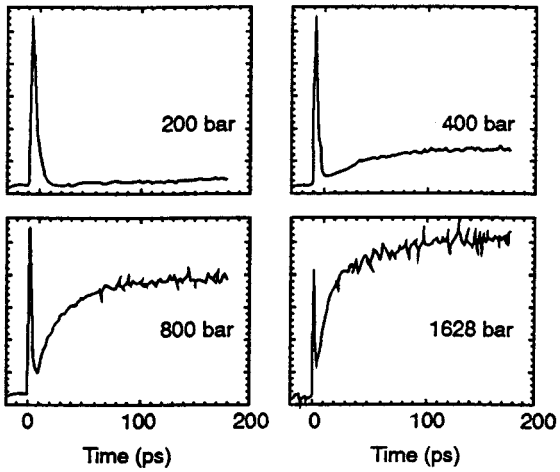

Figure 18. Predissociation and geminate recombination in argon. Experimentally observed transients for iodine dissolved in argon at a temperature of 293 K and at pressures between 200 and 1628 bar. (Reprinted from ref 71. Copyright 1996 American Chemical Society.)

van der Waals complexes. The solid line is a reinterpretation of the data by Combes et al.[54] and includes chemical complexation *and* clustering corrections incorporating ethane isothermal compressibility; however, as discussed in section II.A, there is now considerable evidence[8,12] that local solvent density enhancements, clustering, is not driven by critical properties such as κ_T. Gas-phase clusters and van der Waals complexes have also been proposed to explain recombination reaction turnover from the gas-phase termolecular range to diffusion control at unexpectedly low densities and other anomalous behavior. A more complete description of elementary reactions in the gas−liquid transition are found in the reviews of Harris;[76] and Schroeder and Troe;[77] and the recent investigations of Zewail (vide infra).

2. Femtochemistry of Iodine

Zewail and co-workers[78−80] have recently presented a comprehensive report on their investigations of the femtosecond dynamics of the dissociation and recombination of iodine in the gas-to-liquid transition region. The use of wavelength-tunable femtosecond lasers with fluorescence detection allowed Zewail and co-workers to probe the elementary reaction dynamics of I_2 in real time. Studies in the rare-gas solvents helium, neon, argon, and krypton were performed at solvent densities that spanned from the ideal gas-phase limit to liquidlike fluid. The researchers investigated (1) the impact of solute−solvent interactions on the coherence of the wave packet nuclear motion, (2) the collision-induced predissociation of the B state, and (3) the geminate recombination of the atomic fragments and the subsequent vibrational energy relaxation within the A/A′ states. Figure 18 presents an example of the experimental results for I_2 in argon at 293 K.[79] The short time-scale decay represents the B state decay process of predissociation induced through iodine−solvent collisions. The slower rise in fluorescence signal is attributed to geminate recombination. Figure 19 presents a model description of the processes.[79] After predissociation, the iodine atoms separate on the repulsive potential

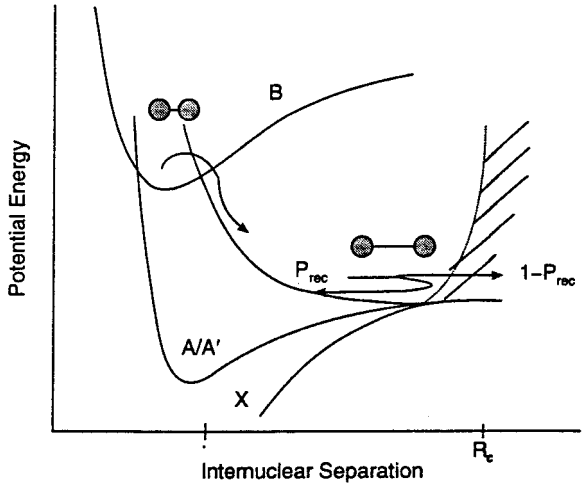

Figure 19. Model description of predissociation and geminate recombination of iodine in supercritical rare gases. After predissociation, the iodine atoms separate on the repulsive potential and transfer their excess energy to the solvent. (Reprinted from ref 78. Copyright 1996 American Chemical Society.)

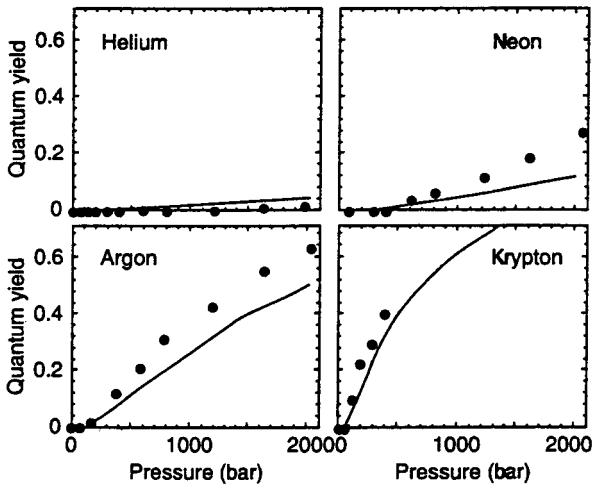

Figure 20. Comparison of experimentally determined quantum yields for geminate recombination with theoretical values from a diffusion-based model (see text). (Reprinted from ref 78. Copyright 1996 American Chemical Society.)

and transfer excess energy to the solvent. When the iodine atoms reach the encounter radius (R_c) there is a finite probability (p_{rec}) for breaking through the solvent barrier. The amplitude of the recombination signal presented in Figure 18 reflects the solvent density dependent probability for geminate recombination onto the A/A′ states. The authors describe two types of geminate caging. Primary or "in-cage" recombination is an ultrafast process in which energy transfer to the first solvent shell will occur. In the high pressure (2500 bar) region this occurs on the subpicosecond time scale. Secondary recombination corresponds to initial breakout followed by reencounter of the original fragments. Experiments indicate that decreasing solvent density increases the probability for breaking out of the solvent cage, while also influencing the distribution function of recombination. Figure 20 presents the quantum yields for geminate recombination,[79] along with values (solid lines) predicted from the diffusion-based model of

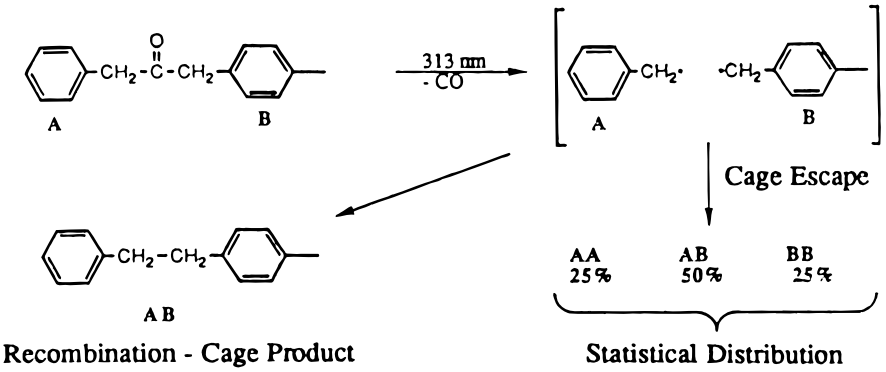

Figure 21. Mechanism of the cage effect for the photolysis of 1-(4-methylphenyl)-3-phenyl-2-propanone. (Reprinted from ref 54. Copyright 1992 American Chemical Society.)

Otto, Schroeder, and Troe.[75] It should be noted that Zewail's SCF experiments were mainly performed at temperatures well removed from the T_c of the rare-gas solvents. In an accompanying paper,[78] MD simulations were used to explore the microscopic influence of solvent under simulated experimental conditions. The results are also compared to previous molecular beam/femtosecond investigations[81] of caging effects in discrete argon clusters, $I_2 \cdot Ar_n$ ($n \approx 8-40$).

3. Photolysis of Dibenzyl Ketones

Fox, Johnston, and co-workers[82] have investigated solvent cage effects on the Norrish type I photochemical cleavage of unsymmetrical dibenzyl ketones in SC CO_2 and ethane. This photoinduced free radical fragmentation reaction is known to produce observable cage effects in micelles and rigid molecular assemblies. The cage effect mechanism is presented in Figure 21. Photolysis of ketone produces distinguishable benzyl radicals A and B. In-cage radical recombination would produce the AB bibenzyl product, whereas cage escape will produce a statistical 1:2:1 distribution of AA, AB, BB coupling products. The fraction of cross-coupling product AB was found to be 50% and independent of pressure (solvent density). These experiments were important in that they were the first chemical experiments specifically designed to test the integrity of SCF clusters and to demonstrate that SCF clusters are not micellelike in nature. In a review[54] of the work the authors reported that "solvent−solute clusters do not present any unusually rigid cage effects to this photolysis compared with liquid solutions". There is an important distinction in regard to existence and detection of solvent cages. Solvent cages will exist in SCFs as they do in normal liquids, however, their influence on chemical reactivity will only be observed when an in-cage process occurs on a shorter (or comparable) time scale than the cage-escape process. It should be noted that photodecomposition of unsymmetrical DBK in normal liquids also results in a 1:2:1 statistical distribution of photoproducts. Furthermore, the reason there is no observable cage effect for this reaction in SCFs is the same for normal liquids. Benzyl radicals A and B are not formed within the same solvent cage. A step-by-step mechanism for the photodecomposition of DBK is presented in Scheme 3, where ISC means intersystem crossing. The mechanism presented in Figure 21 does not account for the time required to produce benzyl radicals A + B. Specifically, the decarbonylation process (step 4 in Scheme 3) is implied to be instantaneous. However, the rate constant for decarbonylation of phenylacetyl radical is reported to be $(5-9) \times 10^6$ s^{-1} in normal liquids at room temperature.[83] Therefore, the second benzyl radical is formed approximately 100 ns following initial Norrish I fragmentation. As a result the AB product is solely formed in a nongeminate diffusion-controlled recombination process as described above.

Scheme 3

$$(PhCH_2)_2C{=}O \xrightarrow{h\nu} (PhCH_2)_2C{=}O^{1*} \quad (1)$$

$$(PhCH_2)_2C{=}O^{1*} \xrightarrow{ISC} (Ph\dot{C}H_2)_2C{=}O^{3*} \quad (2)$$

$$(PhCH_2)_2C{=}O^{3*} \rightarrow Ph\dot{C}H_2 + PhCH_2\dot{C}{=}O \quad (3)$$

$$PhCH_2\dot{C}{=}O \xrightarrow{k_{-CO}} Ph\dot{C}H_2 + CO \quad (4)$$

$$2Ph\dot{C}H_2 \xrightarrow{2k_T} PhCH_2CH_2Ph \quad (5)$$

Brennecke, Chateauneuf, and co-workers[41] have used LFP to directly measure step 4 in Scheme 3, the phenylacetyl radical decarbonylation rate, in SC CO_2, ethane and CHF_3. Fragmentation rate constants ($(1-2) \times 10^7$ s^{-1}) were similar to those observed in normal liquids, and the reaction was not influenced by changes in the bulk physical properties of those solvents.

The possible influence of a SCF cage effect on the geminate radical pairs produced in step 3 of the DBK decomposition reaction (Scheme 3) was also investigated. No cage or solvent density effect was observed. This result is expected; however, since spin selection rules demand formation of a triplet geminate radical pair, and in-cage radical−radical recombination would require ISC to a singlet radical pair prior to product formation. In normal nonviscous solvents, cage escape of the initial radical pair formed in step 3 is >95%. This result is in agreement with Fox, Johnston, and co-workers,[54,82] who found no change in DBK decomposition quantum yield with change in SCF density. The results are also consistent with SCF cluster lifetime estimates.

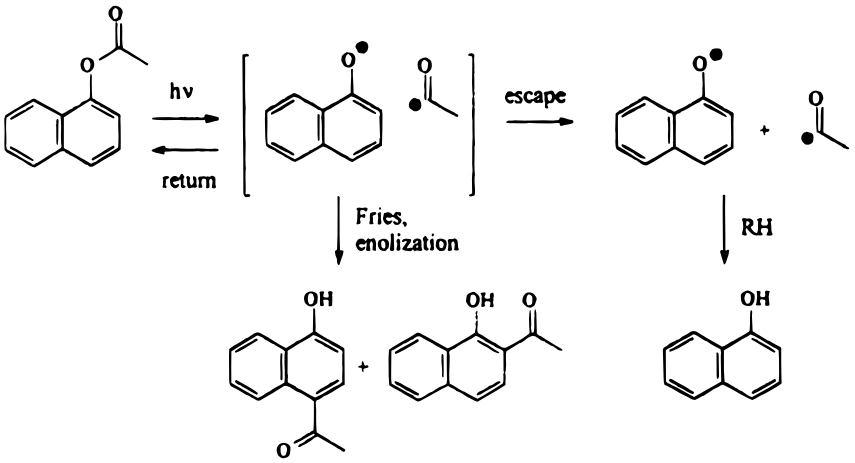

Figure 22. Photo-Fries rearrangement reaction of 1-naphthyl acetate. (Reprinted from ref 85. Copyright 1995 American Chemical Society.)

4. Norrish Type I and Type II Reactions

Morgenstern and Tumas[84] studied the Norrish Type I and II photochemistry of butyrophenone and α,α-dimethylbutyrophenone in supercritical CO_2 at 60 °C at densities well above the critical density. In this regime, they found that the Norrish I/II ratio was well modeled by Troe's theory; in other words, it was solely determined by viscosity. The elimination-to-cyclization ratio of butyrophenone proved somewhat more sensitive to pressure than in conventional solvents (hexane), but here too, the degree of tunability was sharply limited. These authors interpreted their results as suggesting that dense supercritical carbon dioxide exhibits few novel solvation effects and essentially behaves like a conventional nonpolar solvent.

5. Photo-Fries Rearrangement

Weedon and co-workers[85] have investigated the photo-Fries rearrangement of 1-naphthyl acetate in SC CO_2 mixtures. This photofragmentation reaction proceeds through the excited singlet-state manifold to produce a short-lived singlet radical pair (Figure 22), estimated to have a lifetime of 25 ps. Therefore, the ratio of cage-escape product (naphthol) to in-cage Fries rearrangement products (2- and 4-acetylnaphthol) may be used as an effective probe of short-lived solvent cages. Figure 23 presents the pressure dependence ratio of in-cage to cage-escape products in liquid CO_2 and SC CO_2. The influence of the solvent cage in liquid CO_2 is comparable to that observed in normal liquids; however, a dramatic 3-fold increase in the in-cage products is observed under SC conditions at lower bulk densities. Since fragmentation is nearly instantaneous, one may speculate that the radical pair is influenced by the increased local density developed by solute/solvent interaction of the acetate precursor.

6. Chlorine Atom Cage Effects

Tanko and co-workers have recently reported that SC CO_2 may be used as an environmentally benign alternative to CCl_4, CFCs, and benzene for free radical bromination reactions.[86−88] Reaction yields, times, and selectivities, in SC CO_2, were found to be

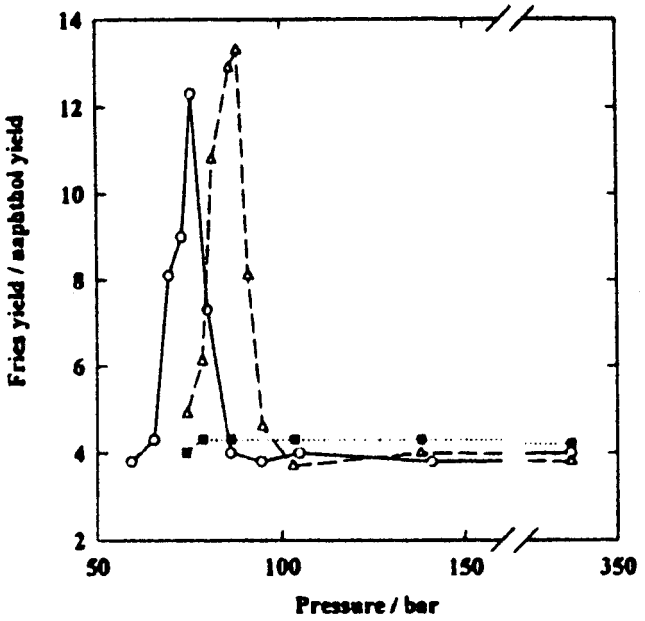

Figure 23. Pressure dependence of the ratio of the photo-Fries product yield for the photolysis of 1-naphthyl acetate (1.80×10^{-3} M): $T = 27$ °C (●); $T = 35$ °C (○); $T = 47$ °C (△). (Reprinted from ref 85. Copyright 1995 American Chemical Society.)

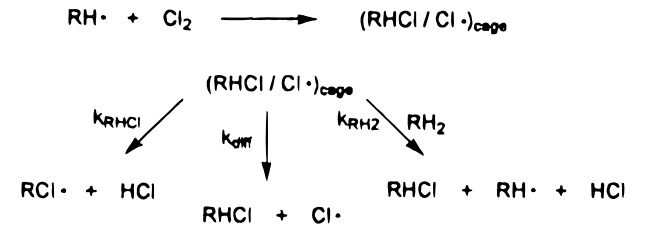

Figure 24. Hydrocarbon free radical chlorination mechanism. (Reprinted from ref 88. Copyright 1996 American Chemical Society.)

analogous to the conventional solvents. Tanko et al.[88] have also recently reported the viscosity-dependent behavior of geminate caged pairs in the free radical chlorination of cyclohexane in SC CO_2. Figure 24 presents the scheme for the photoinduced free radical chain process. During the reaction, chlorine atom abstraction from Cl_2 by cyclohexyl radical produces an alkyl halide/Cl$^{\bullet}$ geminate caged pair. The caged

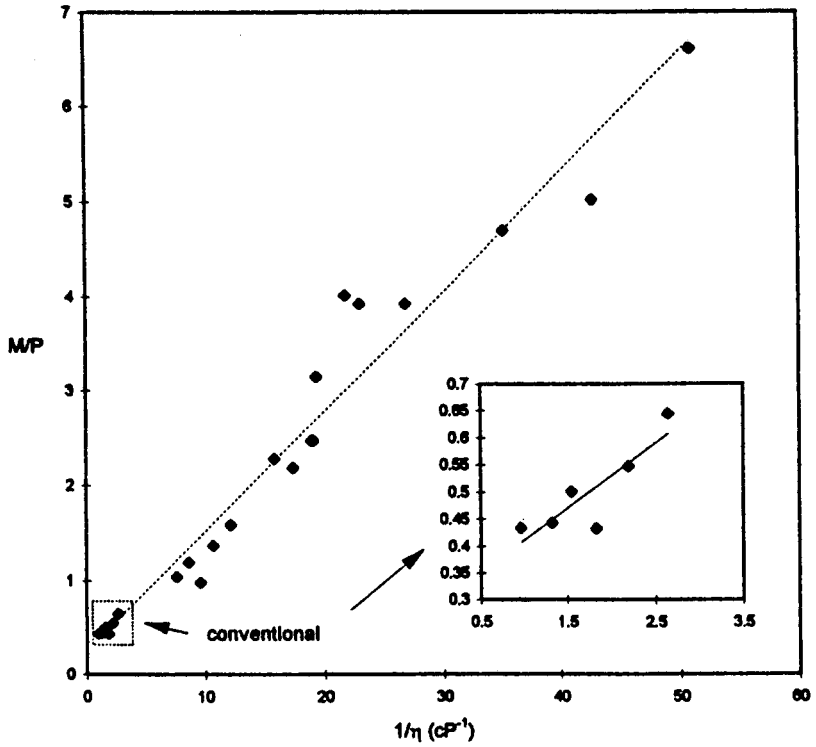

Figure 25. Ratio of mono- to polychlorides produced in the free radical chlorination of cyclohexane in conventional and supercritical fluid solvents as a function of inverse viscosity (40 °C). (Reprinted from ref 88. Copyright 1996 American Chemical Society.)

pair may diffuse apart, or Cl• may undergo a second in-cage H-abstraction from the alkyl chloride, or abstract a hydrogen from cyclohexane molecules contained in the cell wall. The ratio of mono- to polychlorinated products (M/P) may be used to probe cage processes. The M/P ratio was found to vary dramatically with pressure in SC CO_2. The M/P ratio increased significantly at lower CO_2 pressures (solvent density). Since polychlorides are in-cage products, the results reasonably indicate that the cage effect becomes less important at lower fluid densities. The results were presented in terms of the Noyes model, which predicts that the efficiency of cage escape should vary linearly with the inverse of bulk viscosity ($1/\eta$). The SC CO_2 results are presented in Figure 25, along with M/P values obtained in some conventional liquids. Interestingly, these results indicate that the free radical chain process is adequately described using the bulk physical properties of the solvent, i.e., η, with no apparent influence of local effects. It is possible that radical pair formation and dissociation is significantly faster than the time required for an equilibrated solvation.

It is worth noting that in this and previous works, Tanko et al.[86−88] address the important issue of radical/solvent complexation. Complexation may have dramatic influence on selectivity in free radical reactions. McHugh[89] first reported the use of SC CO_2 as a solvent for a free radical chain reaction (the autoxidation of cumene). No unusual effects attributed to solvent complexation were observed. Subsequent studies of carbon-centered free radicals have supported this initial finding;[41,54,82] however, halogen atoms are known to have a propensity to form molecular adducts.[90,91] Tanko et al.[86−88] have investigated selectivities in the competitive bromination of toluene and ethyl benzene[87] and soon will publish results of selectivity of a competitive chlorination reaction. In each case, results nearly identical to conventional halogenation solvents were obtained which strongly suggest free bromine atom and free Cl• as the chain carriers.

In a related study, Fischer and co-workers[92] have recently reported the use of EPR to detect transient free radicals in supercritical liquids solvents, such as toluene and 2-propanol. A variety of radicals were produced by photolytic methods. Radical termination constants, $2k_t$, were determined and k_t was found to be proportional to T/η in liquid, as well as, at supercritical conditions. The reported experimental methodologies are an extension of the earlier work of Livingston et al.[93] who used EPR to observe benzyl radical production and reactivity in the pyrolysis of hydrocarbons in supercritical benzene, toluene, and other high-temperature solvent mixtures. These results are consistent with experimental results and a diffusion-based model of Otto, Schroeder, and Troe[75] (vide supra). The results are also consistent with the other diffusion-controlled reactions[38,41] investigated in SCF at $\rho_r > 1$.

Klein and co-workers[94] have also used transition-state theory to interpret the effect of pressure on the overall reaction rate of benzyl phenyl ether pyrolysis in SC toluene. Phase behavior effects, diffusional limitations, electrostatic interactions, and cage effects were considered for the free radical chain decomposition. It was acknowledged that varying diffusion coefficients from gaslike to liquidlike can change the effective rate of elementary reaction steps. In related work, Sigman and Leffler[95,96] indicated that the

recombination of PhN=N• and triphenyl methyl radical was not important in the decomposition of phenylazotriphenylmethane.[95] Carboxy inversion reactions were observed, however, in the decomposition of diacyl peroxides in SC CO_2.[96] In the latter case, the reactions were attributed to nonradical alkyl group rearrangement and CO_2 exchange.

E. Other Important Reactions and Directions

Although somewhat removed from the scope of this review, polymerization reactions are an important area of SCF technology. The polymerization of ethylene to polyethylene is a well-known commercial application of SCF technology.[97] Spectroscopic and mechanistic studies have also been important in this field. For example, the groups of Ehrlich[98] and Buback[99] have used in situ spectroscopic measurements to determine the absolute rate constants for the polymerization of ethylene by the rotating sector method, and ethylene monomer conversions using time-resolved IR, respectively. For related discussion also see the recent review of Buback.[99c]

In 1992, DeSimone[100a] and co-workers reported the first successful homogeneous free radical polymerization in an inert, nonreacting SCF. They demonstrated that a series of highly fluorinated acrylic monomers could be successfully polymerized to form a variety of fluorinated homopolymers and copolymers, with nonfluorinated comonomers, using homogeneous polymerization methods in SC CO_2. In these studies the thermal decomposition of the common free radical initiator, 2,2-azobis(isobutyronitrile) (AIBN) was investigated. The decomposition rate and initiation efficiency of AIBN in SC CO_2 was studied as a function of temperature and pressure and characterized using solvatochromic measurements and modeled using Kirkwood solution theory. The decomposition rate of AIBN was found to be 2.5 times slower in SC CO_2 than in benzene; however, the initiation efficiency was found to be ca. 1.5 times higher than in benzene and invariant over the 138−345 bar pressure range studied. The former result was attributed to the lower dielectric constant of CO_2 compared to benzene at comparable temperatures and pressures. The later observation was attributed to the lower viscosity of CO_2 compared to benzene, and the invariance to the relatively small pressure range examined. The authors also reported that there was no free radical reactivity with the SC solvent, and in turn SC CO_2 should be considered an acceptable solvent to conduct free radical reactions.[100] This group has also demonstrated the use of SC CO_2 as replacements for chlorofluorocarbons in the synthesis of fluorinated telomers.[101]

Recently, Odell and Georges[102] have also described the use SC CO_2 as a solvent for living free radical polymerizations (LFRP). This type of polymerization uses a stable nitroxide free radical, such as TEMPO, and the concept of reversible termination. These systems can provide polymers of narrow polydispersity, less than 1.3, via controlled, stepwise growth. A valuable attribute of LFRP is the potential to form well-defined block copolymers. The authors suggest that SCF technology may provide an additional benefit of producing block polymers in the absence of conventional solvents and without additional purification beyond the extraction of unreacted monomer of an earlier block.

Another exciting new area of research is the application SCFs as solvents with more conventional synthetic methodologies. For example, Beckman, Curran, and co-workers[103] have recently reported preliminary results of the use of a perfluorinated tin hydride reagent, $(C_6F_{13}CH_2CH_2)_3SnH$ (tris(perfluorohexylethyl)tin hydride), in the free radical initiated reduction of alkyl and aryl halides with SC CO_2 as the reaction medium. For some reactions a direct comparison between the perfluorinated tin hydride and tributyl tin hydride $(Bu)_3SnH$ were performed; however, the results were highly dependent on the alkyl or aryl halide. Solutions of bromoadamantane (0.05 M, 0.85 mmol), 10% AIBN, and either $(Bu)_3SnH$ (1 mmol) or perfluorinated tin hydride (1 mmol) heated for 3 h at 90 °C at 4000 psig, both consumed the bromide and formed adamantane in 88 and 90% yields, respectively. However additional products were observed in the $(Bu)_3SnH$ system. It was noted that the $(Bu)_3SnH$ mixtures were not homogeneous even at 7000 psig. Also, in a control experiment with AIBN, $(Bu)_3SnH$ was found to react with CO_2 to form tin formate, $(Bu)_3SnOC(O)H$. In contrast, the perfluorinated tin hydride did not produce the corresponding formate and was recovered unchanged. On the other hand, the reduction of a primary iodide and steroidal iodide, bromide, and phenyl selenide gave nearly identical results using either hydride. In these last reactions no carboxylated products were observed. In contrast, reduction of 9-iodoanthracene with the fluorous tin hydride yielded 71% anthracene and 10% 9-anthracenecarboxylic acid, presumably from free radical carboxylation. Also of interest, free radical "clock" cyclization reactions, e.g., reduction of 1,1-diphenyl-6-bromo-1-hexene with fluorous tin hydride resulted in 87% of the 5-*exo* cyclized product and 7% of the reduced product. This was unexpected since in normal liquids hydrogen transfer cannot compete with cyclization. The authors suggest the observation is due to higher diffusivity in SCFs compared to normal liquids. The possibility of phase separation was also not firmly ruled out.

Finally, electron-transfer reactivity in SCFs is a new area that may prove very useful in understanding solvation and discerning mechanisms. The first report of electron-transfer reactivity in SCFs investigated the reaction between biphenyl radical anion and pyrene in SC ethane using pulse radiolysis.[104] The authors attempted to determine the pressure dependence of the solvent reorganization energy by the difference between the experimental values and the prediction of the diffusion-controlled rate from SE/D. The differences were within the accuracy of the SE/D predictions,[44] so the conclusions they reach should be taken only qualitatively. However, the study emphasizes the great potential that electron-transfer reactivity has for probing solvation in SCF solutions. In a more recent study[105] the reaction of benzophenone triplet with either triethylamine or 1,4-diazabicyclo[2.2.2]octane (DABCO) was investi-

gated in SC CO_2 and SC ethane. Although the reactions are close to diffusion control in liquids, they occur well below diffusion control in supercritical fluids. Thus, investigation in SCFs have brought to light aspects of the mechanism of electron transfer that were not readily apparent in liquid solution. As a result, electron-transfer reactivity in SCFs holds promise for elucidating fundamentals of both SCF solvation and mechanisms of reactions.

IV. Summary

The studies of diffusion-controlled, activated, and equilibrium-limited homogeneous organic reactions in supercritical fluids described in this review lead to several general conclusions. First, the primary influences on reaction rates, selectivities, and mechanisms are the bulk physical properties of the fluid, which can be varied continuously from gaslike to liquidlike. Dependent upon the particular reaction, the bulk property of importance may be the solution density, the viscosity, or, perhaps, the dielectric constant. Second, local solvation in the form of local density augmentation and local composition enhancements can influence reactivity but this depends on the relative time scales of the reaction and solvation processes. For example, local density augmentation does not affect translational diffusion since the time that the solvent "cluster" maintains its integrity is short compared to the time required for translation.[26,36,41] The solvent shells do not maintain their integrity long enough to produce cage effects in the decomposition of dibenzyl ketones.[41,82] On the other hand, the time scale of the local solvation shell is sufficient to increase the encounter time of nitroxide radicals which results in an enhanced spin-exchange rate.[35] Local composition enhancements can increase the rates of reactions with activation barriers, and since these reactions are slow it is the long time-averaged value of the local composition that one would expect to be important.[24,26,27,54] Third, the specific mechanism of the reaction is very important in determining how both bulk properties and local phenomenon might influence the reaction rate or selectivity. The mechanism of the reaction determines on which aspects of the bulk or local properties in SCFs it will report. Finally, there is tremendous opportunity for conducting all types of chemistry in SCFs. Many of these reactions will elicit new information on both local and bulk solvent effects on reaction rates and selectivites. However, the challenge is to move toward more useful synthetic and practical applications, where both the bulk and local properties of SCF solutions can be used to control reaction rates and product distributions.

V. Acknowledgments

The authors acknowledge support from the following agencies, foundations and institutions: the National Science Foundation, the Environmental Protection Agency, the Department of Energy, the Army Research Office, and the Western Michigan University Faculty Research and Creative Activities Support Fund. In addition, acknowledgment is made to the donors of the Petroleum Research Fund, administered by the American Chemical Society, for partial support of this research.

VI. References

(1) Levelt Sengers, J. M. H. In *Supercritical Fluid Technology: Reviews in Modern Theory and Applications*; Bruno, T. J., Ely, J. F., Eds.; CRC Press: Boca Raton, 1991; p 1.
(2) Tester, J. W.; Holgate, H. R.; Armellini, F. J.; Webley, P. A.; Killilea, W. R.; Hong, G. T.; Barner, H. E. In *Emerging Technologies in Hazardous Waste Management III*; Tedder, D. W., Pohland, F. G., Eds.; ACS Symposium Series 518; American Chemical Society: Washington, DC, 1993; p 35.
(3) (a) Luo, H.; Tucker, S. C. *J. Am. Chem. Soc.* **1995**, *117*, 11359. (b) Luo, H.; Tucker, S. C. *J. Phys. Chem.* **1996**, *100*, 11165. (c) Luo, H.; Tucker, S. C. *J. Phys. Chem. B* **1997**, *101*, 1063. (d) Niemeyer, E. D.; Dunbar, R. A.; Bright, F. V. *Appl. Spectrosc.* **1997**, *51*, 1547. (e) Balbuena, P. B.; Johnston, K. P.; Rossky, P. J. *J. Phys. Chem.* **1996**, *100*, 2706. (f) Balbuena, P. B.; Johnston, K. P.; Rossky, P. J. *J. Phys. Chem.* **1996**, *100*, 2716. (g) Pomelli, C. S.; Tomasi, J. *J. Phys. Chem. A* **1997**, *101*, 3561.
(4) Savage, P. E.; Gopalan, S.; Mizan, T. I.; Martino, C. J.; Brock, E. E. *AIChE J.* **1995**, *41*, 1723.
(5) (a) Jessop, P. G.; Ikariya, I.; Noyori, R. *Nature* **1995**, *368*, 231. (b) Jessop, P. G.; Hsiao, Y.; Ikariya, T.; Noyori, R. *J. Am. Chem. Soc.* **1996**, *118*, 344. (c) Jessop, P. G.; Ikariya, T.; Noyori, R. *Organometallics* **1995**, *14*, 1510. (d) Kazarian, S. G.; Poliakoff, M. *J. Phys. Chem.* **1995**, *99*, 8624. (e) Sun, X. Z.; George, M. W.; Kazarian, S. G.; Nikiforov, S. M.; Poliakoff, M. *J. Am. Chem. Soc.* **1996**, *118*, 10525. (f) Banister, J. A.; Cooper, A. I.; Howdle, S. M.; Jobling, M.; Poliakoff, M. *Organometallics* **1996**, *15*, 1804. (g) Sun, X. Z.; Grills, D. C.; Nikiforov, S. M.; Poliakoff, M.; George, M. W. *J. Am. Chem. Soc.* **1997**, *119*, 7521. (h) Lee, P. D.; King, J. L.; Seebald, S.; Poliakoff, M. *Organometallics* **1998**, *17*, 524. (i) Ji, Q.; Eyring, E. M.; van Eldik, R.; Johnston, K. P.; Goates, S. R.; Lee, M. L. *J. Phys. Chem.* **1995**, *99*, 13461. (j) Ji, Q.; Lloyd, C. R.; Eyring, E. M.; van Eldik, R. *J. Phys. Chem. A* **1997**, *101*, 243.
(6) Kim, S.; Johnston, K. P. *Ind. Eng. Chem. Res.* **1987**, *26*, 1206.
(7) McRae, E. G. *J. Phys. Chem.* **1957**, *61*, 562.
(8) Carlier, C.; Randolph, T. W. *AIChE J.* **1993**, *39*, 876.
(9) Brennecke, J. F.; Tomasko, D. L.; Peshkin, J.; Eckert, C. A. *Ind. Eng. Chem. Res.* **1990**, *29*, 1682.
(10) Schwarzer, D.; Troe, J.; Votsmeier, M.; Zerezke, M. *J. Chem. Phys.* **1997**, *107*, 8380.
(11) (a) Sun, Y. P.; Bennett, G.; Johnston, K. P.; Fox, M. A. *Anal. Chem.* **1992**, *64*, 1763. (b) Sun, Y. P.; Bennett, G.; Johnston, K. P.; Fox, M. A. *J. Phys. Chem.* **1992**, *96*, 10001. (c) Sun, Y. P.; Bennett, G.; Johnston, K. P.; Fox, M. A. *J. Am. Chem. Soc.* **1992**, *114*, 1187. (d) Sun, Y. P.; Bunker, C. E. *Ber. Bunsen-Ges. Phys. Chem.* **1995**, *99*, 976.
(12) Knutson, B. L.; Tomasko, D. L.; Eckert, C. A.; Debenedetti, P. G.; Chialvo, A. A. In *Supercritical Fluid Technology*; Bright, F. V., McNally, M. E. P., Eds.; ACS Symposium Series 488; American Chemical Society: Washington, DC, 1992; p 60.
(13) Zhang, J.; Lee, L. L.; Brennecke, J. F. *J. Phys. Chem.* **1995**, *99*, 9268.
(14) (a) Schwarzer, D.; Troe, J.; Votsmeier, M.; Zerezke, M. *Ber. Bunsen-Ges. Phys. Chem.* **1997**, *101*, 595. (b) Schwarzer, D.; Troe, J.; Votsmeier, M.; Zerezke, M. *J. Chem. Phys.* **1996**, *105*, 3121.
(15) Kauffman, J. F. *Anal. Chem. News Features* **1996**, April 1, 248 A.
(16) Anderton, R. M.; Kauffman, J. F. *J. Phys. Chem.* **1995**, *99*, 13759.
(17) Heitz, M. P.; Bright, F. V. *J. Phys. Chem.* **1996**, *100*, 6889.
(18) (a) Kajimoto, O.; Futakami, M.; Kobayashi, T.; Yamasaki, K. *J. Phys. Chem.* **1988**, *92*, 1347. (b) Morita, A.; Kajimoto, O. *J. Phys. Chem.* **1990**, *94*, 6420.
(19) Wu, R. S.; Lee, L. L.; Cochran, H. D. *Ind. Eng. Chem. Res.* **1990**, *29*, 977.
(20) Petsche, I. B.; Debenedetti, P. G. *J. Chem. Phys.* **1989**, *91*, 7075.
(21) Kim, S.; Johnston, K. P. *AIChE J.* **1987**, *33*, 1603.
(22) Yonker, C. R.; Smith, R. D. *J. Phys. Chem.* **1988**, *92*, 2374.
(23) Ellington, J. B.; Park, K. M.; Brennecke, J. F. *Ind. Eng. Chem. Res.* **1994**, *33*, 965.
(24) Roberts, C. B.; Chateauneuf, J. E.; Brennecke, J. F. *AIChE J.* **1995**, *41*, 1306.
(25) (a) Schulte, R. D.; Kauffman, J. F. *J. Phys. Chem.* **1994**, *98*, 8793. (b) Schulte, R. D.; Kauffman, J. F. *J. Phys. Chem.* **1995**, *49*, 8793.
(26) Zhang, J.; Roek, D. P.; Chateauneuf, J. E.; Brennecke, J. F. *J. Am. Chem. Soc.* **1997**, *119*, 9980.
(27) Roberts, C. B.; Zhang, J.; Chateauneuf, J. E.; Brennecke, J. F. *J. Am. Chem. Soc.* **1995**, *117*, 6553.
(28) (a) Randolph, T. W.; Blanch, H. W.; Prausnitz, J. M. *AIChE J.* **1988**, *34*, 1354. (b) Ganapathy, S.; Randolph, T. W.; Carlier, C.; O'Brien, J. A. *Intl. J. Thermophysics* **1996**, *17*, 471.
(29) (a) Chatterjee, P.; Bagchi, S. *J. Chem. Soc., Faraday Trans.* **1990**, *86*, 1785. (b) Chatterjee, P.; Bagchi, S. *J. Phys. Chem.* **1991**, *95*, 3311. (c) Acree, W. E., Jr.; Wilkins, D. C.; Tucker, S. A. *Appl. Spectrosc.* **1993**, *47*, 1171. (d) Phillips, D. J.; Brennecke. J. F. *Ind. Eng. Chem. Res.* **1993**, *32*, 943. (e) Carre, O. R.; Phillips, D. J.; Brennecke, J. F. *Ind. Eng. Chem. Res.* **1994**, *33*, 1355.

(30) Evans, M. G.; Polanyi, M. *Trans. Faraday Soc.* **1935**, *31*, 875.
(31) Hamann, S. D.; Bradley, R. S. *High-Pressure Physics and Chemistry*; Academic Press: London, 1963; Vol. 2, p 163.
(32) Eckert, C. A.; Ziger, D. H.; Johnston, K. P.; Kim, S. *J. Phys. Chem.* **1986**, *90*, 2738.
(33) Hirschfelder, J. O.; Curtiss, C. F.; Bird, R. B. *Molecular Theory of Gases and Liquids*; Wiley: New York, 1954.
(34) Ganapathy, S.; O'Brien, J. A.; Randolph, T. W. *AIChE J.* **1995**, *41*, 346.
(35) (a) Zagrobelny, J.; Betts, T. A.; Bright, F. V. *J. Am. Chem. Soc.* **1992**, *114*, 5249. (b) Zagrobelny, J.; Bright, F. V. *J. Am. Chem. Soc.* **1992**, *114*, 7821. (c) Zagrobelny, J.; Bright, F. V. *J. Am. Chem. Soc.* **1993**, *115*, 701.
(36) Bunker, C. E.; Rollins, H. W.; Gord J. R.; Sun, Y.-P. *J. Org. Chem.* **1997**, *62*, 7324.
(37) Sun, Y.-P.; Bunker, C. E.; Hamilton, N. B. *Chem. Phys. Lett.* **1993**, *21*, 111.
(38) Rice, J. K.; Niemeyer, E. D.; Dunbar, R. A.; Bright, F. V. *J. Am. Chem. Soc.* **1995**, *117*, 5832.
(39) Randolph, T. W.; Carlier, C. *J. Phys. Chem.* **1992**, *96*, 5146.
(40) Saltiel, J.; Atwater, V. W. *Adv. Photochem.* **1988**, *14*, 1.
(41) (a) Roberts, C. B.; Zhang, J.; Brennecke, J. F.; Chateauneuf, J. E. *J. Phys. Chem.* **1993**, *97*, 5618. (b) Roberts, C. B.; Zhang, J.; Chateauneuf, J. E.; Brennecke, J. F. *J. Am. Chem. Soc.* **1993**, *115*, 9576.
(42) Worrall, D. R.; Wilkinson, F. *J. Chem. Soc., Faraday Trans.* **1996**, *92*, 1467.
(43) Bunker, C. E.; Sun, Y. P. *J. Am. Chem. Soc.* **1995**, *117*, 10865.
(44) Liong, K. K.; Wells, P. A.; Foster, N. F. *J. Supercrit. Fluids* **1991**, *4*, 91.
(45) Bunker, C. E.; Sun, Y. P.; Gord, J. R. *J. Phys. Chem. A* **1997**, *101*, 9233.
(46) Johnston, K. P.; Haynes, C. *AIChE J.* **1987**, *33*, 2017.
(47) Paulaitis, M. E.; Alexander, G. C. *Pure Appl. Chem.* **1987**, *59*, 61.
(48) (a) Ikushima, Y.; Saito, N.; Arai, M. *J. Phys. Chem.* **1992**, *96*, 2293. (b) Ikushima, Y.; Ito, S.; Asano, T.; Yokoyama, T.; Saito, N.; Hatakeda, K.; Goto, T. *J. Chem. Eng. Jpn.* **1990**, *23*, 96. (c) Knutson, B. L.; Dillow-Wilson, A. K.; Liotta, C. L.; Eckert, C. A. In *Innovations in Supercritical Fluids*; Hutchenson, K. W., Foster, N. R., Eds.; ACS Symposium Series 608; American Chemical Society: Washington, DC, 1995; p 166.
(49) Renslo, A. R.; Weinstein, R. D.; Tester, J. W.; Danheiser, R. L. *J. Org. Chem.* **1997**, *62*, 4530.
(50) (a) Zhang, J.; Connery, K. A.; Brennecke, J. F.; Chateauneuf, J. E. *J. Phys. Chem.* **1996**, *100*, 12394. (b) Quint, J. R.; Wood, R. H. *J. Phys. Chem.* **1985**, *89*, 380.
(51) (a) Cummings, P. T.; Cochran, H. D.; Simonson, J. M.; Mesmer, R. E.; Karaborni, S. *J. Chem. Phys.* **1991**, *94*, 5606. (b) Cochran, H. D.; Cummings, P. T.; Karaborni, S. *Fluid Phase Equilib.* **1992**, *71*, 1. (c) Cummings, P. T.; Chialvo, A. A.; Cochran, H. D. *Chem. Eng. Sci.* **1994**, *49*, 2735. (d) Cui, S. T.; Harris, J. G. *Chem. Eng. Sci.* **1994**, *49*, 2749. (e) Bennett, G. E.; Rossky, P. J.; Johnston, K. P. *J. Phys. Chem.* **1995**, *99*, 16136. (f) Chialvo, A. A.; Cummings, P. T.; Simonson, J. M.; Mesmer, R. E. *J. Chem. Phys.* **1996**, *105*, 9248. (g) Johnston, K. P.; Bennett, G. E.; Balbuena, P. B.; Rossky, P. J. *J. Am. Chem. Soc.* **1996**, *118*, 6746. (h) Flanagin, L. W.; Balbuena, P. B.; Johnston, K. P.; Rossky, P. J. *J. Phys. Chem. B* **1997**, *101*, 7998. (i) Re, M.; Laria, D. *J. Phys. Chem. B* **1997**, *101*, 10494. (j) Luo, H.; Tucker, S. C. *Theor. Chem. Acc.* **1997**, *96*, 84.
(52) (a) Kajimoto, O.; Sekiguchi, K.; Nayuki, T.; Kobayashi, T. *Ber. Bunsen-Ges. Phys. Chem.* **1997**, *101*, 600. (b) Kajimoto, O.; Nayuki, T.; Kobayashi, T. *Chem. Phys. Lett.* **1993**, *209 (4)*, 357.
(53) Rhodes, T. A.; O'Shea, K.; Bennett, G.; Johnston, K. P.; Fox, M. A. *J. Phys. Chem.* **1995**, *99*, 9903.
(54) Combes, J. R.; Johnston, K. P.; O'Shea, K. E.; Fox, M. A. In *Supercritical Fluid Technology*; Bright, F. V., McNally, M. E. P., Eds.; ACS Symposium Series 488; American Chemical Society: Washington, DC, 1992; p 31.
(55) Hrnjez, B. J.; Mehta, A. J.; Fox, M. A.; Johnston, K. P. *J. Am. Chem. Soc.* **1989**, *111*, 2662.
(56) (a) Kimura, Y.; Yoshimura, Y.; Nakahara, M. *J. Chem. Phys.* **1989**, *90*, 5679. (b) Kimura, Y.; Yoshimura, Y. *J. Chem. Phys.* **1992**, *96*, 3085. (c) Kimura, Y.; Yoshimura, Y. *J. Chem. Phys.* **1992**, *96*, 3824.
(57) Yoshimura, Y.; Kimura, Y. *Chem. Phys. Lett.* **1991**, *181*, 517.
(58) Fulton, J. L.; Yee, G. G.; Smith, R. D. *J. Am. Chem. Soc.* **1991**, *113*, 8327.
(59) Kazarian, S. G.; Gupta, R. B.; Clarke, J. J.; Johnston, K. P.; Poliakoff, M. *J. Am. Chem. Soc.* **1993**, *115*, 11099.
(60) Gupta, R. B.; Combes, J. R.; Johnston, K. P. *J. Phys. Chem.* **1993**, *97*, 707.
(61) Meredith, J. C.; Johnston, K. P.; Seminario, J. M.; Kazarian, S. G.; Eckert, C. A. *J. Phys. Chem.* **1996**, *100*, 10837.
(62) Peck, D. G.; Mehta, A. J.; Johnston, K. P. *J. Phys. Chem.* **1989**, *93*, 4297.
(63) Yamasaki, K.; Kajimoto, O. *Chem. Phys. Lett.* **1990**, *172*, 271.
(64) Akao, K.; Yoshimura, Y. *J. Chem. Phys.* **1991**, *94*, 5243.
(65) Yagi, Y.; Saito, S.; Inomata, H. *J. Chem. Eng. Jpn.* **1993**, *26*, 11.
(66) O'Shea, K. E.; Kirmse, K. M.; Fox, M. S.; Johnston, K. P. *J. Phys. Chem.* **1991**, *95*, 7863.
(67) (a) Tomasko, D. L.; Knutson, B. L.; Pouillot, F.; Liotta, C. L.; Eckert, C. A. *J. Phys. Chem.* **1993**, *97*, 11823. (b) Tomasko, D. L.; Knutson, B. L.; Eckert, C. A.; Haurich, J. E.; Tolbert, L. M. In *Supercritical Fluid Technology*; Bright, F. V., McNally, M. E. P., Eds.; ACS Symposium Series 488; American Chemical Society: Washington, DC, 1992; p 84.
(68) Dillow, A. K.; Hafner, K. P.; Yun, S. L. J.; Deng, F.; Kazarian, S. G.; Liotta, C. L.; Eckert, C. A. *AIChE J.* **1997**, *43*, 515.
(69) Sigman, M. E.; Leffler, J. E. *J. Org. Chem.* **1987**, *52*, 3123.
(70) Aida, T.; Squires, T. G. In *Supercritical Fluids*; Squires, T. G., Paulaitis, M. E., Eds.; ACS Symposium Series 329; American Chemical Society: Washington, DC, 1987; p 58.
(71) Nikowa, L.; Schwarzer, D.; Troe, J.; Schroeder, J. *Ultrafast Phenomena VIII*; Martin, J.-L., Migus, A., Mourou, G. A., Zewail, A. H., Eds.; Springer Series in Chemical Physics, Vol. 55; Springer-Verlag: Berlin, 1993; p 603.
(72) Hara, K.; Kiyotani, H.; Kajimoto, O. *J. Chem. Phys.* **1995**, *103*, 5548.
(73) O'Brien, J. A.; Randolph, T. W.; Carlier, C.; Ganapathy, G. *AIChE J.* **1993**, *39*, 1061.
(74) Franck, J.; Rabinowitch, E. *Trans. Faraday Soc.* **1930**, *30*, 120.
(75) Otto, B.; Schroeder, J.; Troe, J. *J. Chem. Phys.* **1984**, *81*, 202.
(76) Harris, A. L.; Brown, J. K.; Harris, C. B. *Annu. Rev. Phys. Chem.* **1988**, *39*, 341.
(77) Schroeder, J.; Troe, J. *Annu. Rev. Phys. Chem.* **1987**, *38*, 163.
(78) Liu, Q.; Wan, C.; Zewail, A. H. *J. Phys. Chem.* **1996**, *100*, 18666.
(79) Lienau, C.; Zewail, A. H. *J. Phys. Chem.* **1996**, *100*, 18629.
(80) Materny, A.; Lienau, C.; Zewail, A. H. *J. Phys. Chem.* **1996**, *100*, 18650.
(81) Wang, J.-K.; Liu, Q.; Zewail, A. H. *J. Phys. Chem.* **1995**, *99*, 11309.
(82) O'Shea, K. E.; Combes, J. R.; Fox, M. A.; Johnston, K. P. *Photochem. Photobiol.* **1991**, *54*, 571.
(83) (a) Lunazzi, L.; Ingold, K. U.; Scaiano, J. C. *J. Phys. Chem.* **1983**, *87*, 529. (b) Turro, N. J.; Gould, I. R.; Baretz, B. H. *J. Phys. Chem.* **1983**, *87*, 531.
(84) Morgenstern, D. A.; Tumas, W. Submitted to *J. Am. Chem. Soc.*, 1998.
(85) Andrew, D.; Des Islet, B. T.; Margaritis, A.; Weedon, A. C. *J. Am. Chem. Soc.* **1995**, *117*, 6132.
(86) Tanko, J. M.; Balckert, J. F. *Science* **1994**, *263*, 203.
(87) Tanko, J. M.; Balckert, J. F.; Sadeghipour, M. In *Benign by Design*; Anastas, P. T., Farris, C. A., Eds.; ACS Symposium Series 577; American Chemical Society: Washington, DC, 1994; p 98.
(88) Tanko, J. M.; Suleman, N. K.; Fletcher, B. *J. Am. Chem. Soc.* **1996**, *118*, 11958.
(89) Suppes, G. J.; Occhiogrosso, R. N.; McHugh, N. A. *Ind. Eng. Chem. Res.* **1989**, *28*, 1152.
(90) Russell, G. A. *J. Am. Chem. Soc.* **1958**, *80*, 4897.
(91) Chateauneuf, J. E. *J. Am. Chem. Soc.* **1993**, *115*, 1915.
(92) Batchelor, S. N.; Henningsen, B.; Fischer, H. *J. Phys. Chem. A* **1997**, *101*, 2969.
(93) (a) Livingston, R.; Zeides, H. *J. Phys. Chem.* **1983**, *87*, 1086. (b) Livingston, R.; Zeides, H.; Conradi, M. S. *J. Am. Chem. Soc.* **1979**, *111*, 4312.
(94) Wu, B. C.; Klein, M. T.; Sandler, S. I. *Ind. Eng. Chem. Res.* **1991**, *30*, 822.
(95) Sigman, M. E.; Leffler, J. E. *J. Org. Chem.* **1987**, *52*, 1165.
(96) Sigman, M. E.; Barbas, J. T.; Leffler, J. E. *J. Org. Chem.* **1987**, *52*, 1754.
(97) Ehrlich, P.; Mortimer, G. A. *Adv. Polym. Sci.* **1970**, *7*, 386.
(98) (a) Takahashi, T.; Ehrlich, P. *Polym. Prepr.* **1981**, *22*, 203. (b) Takahashi, T.; Ehrlich, P. *Macromolecules* **1982**, *15*, 714.
(99) (a) Brackemann, H.; Buback, M.; Vögele, H.-P. *Makromolecules* **1986**, *187*, 1977. (b) Buback, M.; Huckestein, B.; Leinhos, U. *Macromol. Chem. Rapid Commun.* **1987**, *8*, 473. (c) Buback, M. *Angew. Chem., Int. Ed. Engl.* **1991**, *30*, 641.
(100) (a) DeSimone, J. M.; Guan, Z.; Elsbernd, C. S. *Science* **1992**, *257*, 945. (b) Guan, Z.; Combes, J. R.; Menceloglu, Y. Z.; DeSimone, J. M. *Macromolecules* **1993**, *26*, 2663. (c) DeSimone, J. M.; Maury, E. E.; Menceloglu, Y. Z.; McClain, J. B.; Romack, T. J.; Combes, J. R. *Science* **1994**, *265*, 356.
(101) (a) Combes, J. R.; Guan, Z.; DeSimone, J. M. *Macromolecules* **1994**, *27*, 865. (b) Romack, T. J.; Combes, J. R.; DeSimone, J. M. *Macromolecules* **1995**, *28*, 1724. (c) Romack, T. J.; DeSimone, J. M. *Macromolecules* **1995**, *28*, 8429.
(102) (a) Odell, P. G.; Hamer, G. K. *Polym. Mater. Sci. Eng.* **1996**, *74*, 404. (b) Georges, M. K.; Veregin, R. P. N.; Kazmaier, P. M.; Hamer, G. K.; Saban, M. *Macromolecules* **1994**, *27*, 7228. (c) Odell, P. G.; Verigin, R. P. N.; Michalak, L. M.; Georges, M. K. *Macromolecules*, in press.
(103) Hadida, S.; Super, M. S.; Beckman, E. J.; Curran, D. P. *J. Am. Chem. Soc.* **1997**, *119*, 7406.
(104) Takahashi, K.; Jonah, C. D. *Chem. Phys. Lett.* **1997**, *264*, 297.
(105) (a) Roek. D. P.; Kremer, M. J.; Brennecke, J. F. Proceedings of the Eighth International Conference on Properties and Phase Equilibria for Product and Process Design, April 26−May 1, 1998, Noordwijkerhout, The Netherlands. (b) Roek. D. P.; Kremer, M. J.; Brennecke, J. F.; Roberts, C. B.; Chateauneuf, J. E. *Fluid Phase Equilib.*, accepted for publication, 1998.

CR970035Q